



## Paving the way to a neural fate – RNA signatures in naive and trans-differentiating mesenchymal stem cells

Caroline Diener<sup>a</sup>, Konstantin Thüre<sup>a</sup>, Annika Engel<sup>b,c</sup>, Martin Hart<sup>a</sup>, Andreas Keller<sup>b,c</sup>, Eckart Meese<sup>a</sup>, Ulrike Fischer<sup>a,\*</sup>

<sup>a</sup> Saarland University (USAAR), Institute of Human Genetics, Homburg 66421, Germany

<sup>b</sup> Saarland University (USAAR), Chair for Clinical Bioinformatics, Saarbrücken 66123, Germany

<sup>c</sup> Helmholtz Institute for Pharmaceutical Research Saarland (HIPS), Helmholtz Center for Infection Research (HZI), Saarland University Campus, Saarbrücken 66123, Germany

### ARTICLE INFO

#### Keywords:

Mesenchymal stem cells (MSCs)  
Trans-differentiation  
Neuron  
Time-course  
Transcriptome  
miRnome

### ABSTRACT

Mesenchymal Stem Cells (MSCs) derived from the embryonic mesoderm persist as a viable source of multipotent cells in adults and have a crucial role in tissue repair. One of the most promising aspects of MSCs is their ability to trans-differentiate into cell types outside of the mesodermal lineage, such as neurons. This characteristic positions MSCs as potential therapeutic tools for neurological disorders. However, the definition of a clear MSC signature is an ongoing topic of debate. Likewise, there is still a significant knowledge gap about functional alterations of MSCs during their transition to a neural fate. In this study, our focus is on the dynamic expression of RNA in MSCs as they undergo trans-differentiation compared to undifferentiated MSCs. To track and correlate changes in cellular signaling, we conducted high-throughput RNA expression profiling during the early time-course of human MSC neurogenic trans-differentiation. The expression of synapse maturation markers, including *NLGN2* and *NPTX1*, increased during the first 24 h. The expression of neuron differentiation markers, such as *GAP43* strongly increased during 48 h of trans-differentiation. Neural stem cell marker *NES* and neuron differentiation marker, including *TUBB3* and *ENO1*, were highly expressed in mesenchymal stem cells and remained so during trans-differentiation. Pathways analyses revealed early changes in MSCs signaling that can be linked to the acquisition of neuronal features. Furthermore, we identified microRNAs (miRNAs) as potential drivers of the cellular trans-differentiation process. We also determined potential risk factors related to the neural trans-differentiation process. These factors include the persistence of stemness features and the expression of factors involved in neurofunctional abnormalities and tumorigenic processes. In conclusion, our findings contribute valuable insights into the intricate landscape of MSCs during neural trans-differentiation. These insights can pave the way for the development of safer treatments of neurological disorders.

### 1. Introduction

Mesenchymal Stem Cells (MSCs) serve as a valuable and sustainable source of multipotent cells involved in the regeneration of mesodermal tissues (Hoang et al., 2022; Rohban and Pieber, 2017; Vasanthan et al., 2020). They differentiate into mesodermal cell types, such as osteoblasts, chondrocytes, and adipocytes (Hmadcha et al., 2020). Moreover, MSCs possess the ability to trans-differentiate into various cell types

from outside the mesodermal lineage, such as astrocytes, oligodendrocytes, and neurons. This trans-differentiation process can be induced by *in vitro* stimulation with specific differentiation media (Hermann et al., 2004; Hernandez et al., 2020; Kopen et al., 1999).

The ability of MSCs to develop into specific cell types combined with their ethical advantages over embryonic stem cells highlights their immense potential for therapeutic applications in personalized medicine (Feier et al., 2022; Harris, 2014; Hoang et al., 2022; Volarevic et al.,

**Abbreviations:** HBMSCs, human bone marrow-derived Mesenchymal Stem Cells; CCL2, C-C motif chemokine ligand 2; CNS, Central Nervous System; EM, extracellular matrix; FC, Fold Change; FDR, False Discovery Rate; GO, Gene Ontology; ISCT, International Society for Cellular Therapy; MiRNA, microRNA; HPO, Human Phenotype Ontology; NES, nestin; NPTX1, neuronal pentraxin 1; NSC, neural stem cell; RRNA, ribosomal RNA; TRNA, transfer RNA; R<sub>q</sub>, Relative quantification; TUBB3, β-tubulin III; UC-MSC, umbilical cord-derived Mesenchymal Stem Cell.

\* Corresponding author.

E-mail address: [ulrike.fischer@uks.eu](mailto:ulrike.fischer@uks.eu) (U. Fischer).

<https://doi.org/10.1016/j.ejcb.2024.151458>

Received 23 April 2024; Received in revised form 18 September 2024; Accepted 21 September 2024

Available online 26 September 2024

0171-9335/© 2024 The Author(s).

Published by Elsevier GmbH. This is an open access article under the CC BY license

(<http://creativecommons.org/licenses/by/4.0/>).

2018). The neural trans-differentiation capacity of MSCs has attracted significant interest for therapeutic interventions in neurological injuries and neurodegenerative diseases such as Parkinson's and Alzheimer's disease (Hernandez et al., 2020; Rahbaran et al., 2022). Ongoing clinical trials explore replacing damaged neuronal cells with trans-differentiated MSCs derived from the adult bone marrow (Choudhary et al., 2021; Hernandez et al., 2020; Hoang et al., 2022). To ensure safe use in clinical applications, it is crucial to have a comprehensive understanding on the processes that underlie MSC neural trans-differentiation (Lee et al., 2021; Lukomska et al., 2019; Musial-Wysocka et al., 2019). A thorough characterization could lead to more effective cell therapy approaches (Pittenger et al., 2019). However, the changes in cellular signaling that guide MSCs to their trans-differentiated state are still not fully understood (Choudhary et al., 2021; Hernandez et al., 2020; Lee et al., 2021).

Heterogeneous results have been reported for the molecular characteristics that define the MSC identity (Musial-Wysocka et al., 2019; Pittenger et al., 2019; Wang et al., 2021). A growing body of evidence could help to improve these criteria at the starting-point of the trans-differentiation process (Pittenger et al., 2019). Though, time-course RNA expression data are particularly useful to track and correlate changes in cellular signaling (Bar-Joseph et al., 2012; Diener et al., 2023a, 2020), only a few efforts have been made to decipher the transcriptional restructuring that directs MSCs towards their neuronal fate (Cortes-Medina et al., 2019; Khan et al., 2020), resulting in a disjointed picture of the relevant functional connections. Likewise, limited information is provided on factors that entail long-term therapeutic risks, including the expression of genes that bear tumorigenic potentials (Hernandez et al., 2020; Musial-Wysocka et al., 2019). Neuron-like morphologies can be observed as early as 48 hours after the initiation of the trans-differentiation process (Cortes-Medina et al., 2019; Miao et al., 2017). Based on this, we focused on this early time-window and generated time-resolved RNA expression data during the trans-differentiation of human bone marrow-derived MSCs (hBMSCs). We found relevant changes in cellular signaling that can be linked to the acquisition of neuronal features. Our study also uncovers potential issues that should be acknowledged when assessing the utility of MSC-derived neurons for therapeutic interventions. The transcripts and microRNAs with prominent time-course changes are both provided in an atlas format.

## 2. Materials and methods

### 2.1. Cultivation of human bone marrow derived mesenchymal stem cells (hBMSCs)

Human BMSCs (C-12974) were obtained from PromoCell GmbH (Heidelberg, Germany). The cell samples were derived from femoral head samples of a 66- (lot# 451Z012.3) and a 72-year-old (lot# 475Z010.3) female Caucasian donor, respectively. To strengthen the significance of the results, the RNA analyses were carried out on the cells of one donor and the protein-staining validation on the cells of the other donor, as indicated below. Corresponding cell charges were approved and certified by the supplier with immune staining and flow cytometric analyses. The cells were seeded at a density of 100,000/25 cm<sup>2</sup> flask with Mesenchymal Stem cell Growth Medium (PromoCell) and expanded for 1–2 passages before induction of the trans-differentiation.

### 2.2. Induction of neural trans-differentiation and collection of time-course samples

For neural trans-differentiation the BMSCs (lot# 451Z012.3) were seeded on fibronectin coated flasks and were allowed to reach a cell density of 60–80 % confluence. Once the appropriate confluence was reached, trans-differentiation induction was started by addition of Stem Cell Neurogenic Differentiation Medium (C-28015, PromoCell). Prior to this differentiation induction, the 0 h sample was collected.

Cellular samples were collected from 25 cm<sup>2</sup> culture flasks at 0, 3, 6, 9, 12, 24 and 48 h after addition of Neurogenic Differentiation Medium. Four independent replicates of the time-course experiment were performed resulting in a total of n=28 cell samples that were subject to subsequent RNA expression analyses. For cellular staining analyses, differentiation experiments were repeated with an independent biological replicate of cells (lot# 475Z010.3) and examined for representative time-points.

In a control experiment BMSCs were seeded on flasks with MSC Growth Medium 2 (C-28009, PromoCell). Cellular samples were collected at 0, 3, 6, 24 and 48 h after reaching 60 % confluence.

### 2.3. Staining of neural protein markers and fluorescence microscopy

Trans-differentiation experiments were repeated, to examine protein expression. Representative time-points were selected based on the information from time-course RNA expression data. For immune fluorescence analysis, BMSC were cultivated on fibronectin coated glass slides and allowed to reach 60–80 % confluence. Cells on glass slides for 0 h samples were methanol fixed when they reached 60–80 % confluence. Cells on glass slides for 9 h, 24 h, 48 h, 3 days and 7 days samples were differentiated by addition of Stem Cell Neurogenic Differentiation Medium and methanol fixed at the indicated time-points.

Cells on glass slides were permeabilized using 0.1 % Triton X100 for 15 minutes, blocked with 1 % goat serum for 30 minutes and incubated with primary antibodies: rabbit anti-NP-I 1:100 (Abcam, ab300404); rabbit anti-MCP1 1:50 (Abcam, ab214819); mouse anti-Nestin 1:200 (Abcam, ab18102); rabbit anti-β-III-Tubulin 1:200 (Abcam, ab18207) for one hour. After three PBS washing steps, secondary antibodies were added (goat anti-rabbit-Alexa Fluor 594 to detect NP-I and MCP1; goat anti-mouse-Alexa Fluor 594 and goat anti-rabbit-Alexa Fluor 488 to detect Nestin and β-III-Tubulin) 1:500. Nuclei were counterstained with DAPI.

### 2.4. Total RNA extraction, quantification and quality control

Cellular total RNA was extracted following the manufacturers' instructions from miRNeasy Mini Kit (Qiagen, Hilden, Germany). Concentrations of the isolated samples were determined by NanoDrop™ 2000c Spectrophotometer (Thermo Fisher Scientific Inc., Waltham, MA, USA). RNA integrity was verified using an Agilent 2100 Bioanalyzer instrument with the RNA Nano Kit (Agilent Technologies, Santa Clara, CA, USA).

### 2.5. Analysis of time-resolved RNA expression profiles

miRNA and transcriptome profiles were determined based on the same total RNA samples. High-throughput miRNA and transcriptome expression analyses were conducted as detailed in a previous publication (Diener et al., 2020) using microarray systems from Agilent Technologies (miRNA: Complete Labeling and Hyb Kit with Human SurePrint G3 Unrestricted miRNA arrays (Release 21.0, G4872A); transcriptome: Low Input Quick Amp Labeling Kit and the Gene Expression Hybridization Kit with Human SurePrint G3 Gene Expression Microarrays (V3, G4851C)). For transcriptome analyses, cRNA was purified using RNeasy Mini Kit (Qiagen) and cRNA concentrations were determined with a NanoDrop™ 2000c Spectrophotometer (Thermo Fisher Scientific Inc.).

### 2.6. Validation of time-resolved RNA expression patterns by quantitative reverse transcription polymerase chain reactions (RT-qPCRs)

The total RNA (500 ng) was reverse transcribed to cDNA using the QuantiTect RT Kit, (Qiagen GmbH, Hilden, Germany). For the qPCR analyses, 5 ng of the resulting cDNAs were used together with the SYBR® Green PCR Kit (Qiagen) and with Qiagen QuantiTect assays: *NES* (QT00235781), *NPTX1* (QT00083846), *NLGN2* (QT00007189), *TUBB3*

(QT00083713), *GAP43* (QT00023639), *ITGA5* (QT00080871), *PRSS35* (QT00204113), *ANLN* (QT00011585), *MMP13* (QT00001764). The qPCRs were run on a QuantStudio3™ Real-Time PCR System (Applied Biosystems™, Foster City, USA). Relative expression levels of the analyzed genes were determined with reference to *GAPDH* (Primer Assay: QT00079247) that served as endogenous control. Data evaluation was conducted using the Applied Biosystems™ Analysis Software, Relative Quantification Analysis Module, VERSION 4.3 (Thermo Fisher Scientific Inc.). Due to insufficient sample quantities, only three of the original four time-course replicates were included in the RT-qPCRs analyses. All analyses were conducted in duplicate technical replicates from each of the three biological replicates resulting in six analyses per tested gene and time-point.

In addition to RT-qPCR analysis of differentiated MSCs we investigated BMSCs with RT-qPCR during growth in MSC Maintenance Medium as described above.

### 2.7. Quantitative evaluation of miRNA expression data

For a quantitative evaluation of the miRNA expression data, a previously determined calibration curve (Diener et al., 2020) was applied to the accordingly processed data of the employed microarray analysis system. Using Avogadro's constant and assuming a total amount of 20 pg total RNA per cell (Monaco et al., 2012; Tang et al., 2019), absolute miRNA expression values [molecules/cell] were extrapolated.

### 2.8. Microarray processing and statistical comparisons

Microarray image analysis was conducted using Feature Extraction software (Agilent Technologies, Santa Clara, CA, USA). Absence of gene expression was specified by no detection throughout the microarray image analysis and excluded from further analysis. The raw microarray data were concatenated into one matrix using Python in version 3.7 with the package "NumPy" in version 1.16.4. Further, the data were background corrected, quantile normalized and log<sub>2</sub>-transformed with R in version 3.5.1 with the packages "data.table" (v 1.12.0) and "Bioconductor-preprocesscore" (v 1.46.0). The processing was applied for the transcriptome and miRnome data, respectively. To determine medians, fold changes and t-tests, while obtaining the DEG analysis, R in version 4.0.3 was used with the package "data.table" in version 1.14.2. P-values were adjusted using the Benjamini-Hochberg method. An adjusted p-value of ≤ 0.05 was considered statistically significant. As for the pair-wise comparisons between the four replicated time-course experiments, correlation coefficients (Pearson) were determined by using GraphPad Prism software in version 10.1.1 (Graphpad Software, Inc.). Unless otherwise stated, high expression levels were defined by a log<sub>2</sub> expression >7.

### 2.9. Clustering analyses

For the trajectory analysis of the transcriptomic data the expression values were standardized via z-scores by transcript (mRNA). The clustering of the transcripts by their time trajectory was performed using the fuzzy c-means algorithm. The optimal number of clusters was selected by investigating the minimum centroid distance measure. The miRNA trajectory analysis was accomplished analogously. R in version 4.1.2 was used with the packages data.table (v 1.14.2) and Mfuzz (v 2.54.0), the last package was used for z-scoring and clustering.

### 2.10. Integration of known miRNA-target interactions

Lists of known miRNA-target relations were obtained from the miRTargetLink 2.0 online tool (Kern et al., 2021a) performing a search on the designated miRNAs under the criterion of a "strong validation" typus for the evidenced target interaction. Results were compared with the list of prominently altered mRNA transcripts.

### 2.11. Determination of functional interactions and pathway enrichment analyses

Functional interactions were analyzed by and exported from STRING database (version 11.5; <https://string-db.org/>) (Szklarczyk et al., 2021), excluding text-mining from the selection of active interaction sources and hiding the disconnected nodes. Pathway enrichment analyses were conducted by the embedded feature of corresponding STRING interaction networks ("Functional enrichments in your network"). In designated cases, subnetworks were represented for the enrichment of certain cellular processes.

## 3. Results

### 3.1. Experimental setup and quality control

Towards the establishment of neuron-like phenotypes, the cellular processes during the first two days of MSC trans-differentiation are yet to be deciphered. We conducted a detailed time-course RNA expression profiling (Fig. 1A) during the early trans-differentiation of hBMSCs. Cells were grown on fibronectin coated flasks and time-course samples were collected at 0, 3, 6, 9, 12, 24 and 48 h after addition of a standard commercial neurogenic differentiation medium. High quality of the RNA time-course samples was confirmed by RNA integrity numbers (RIN) ranging from 9.3 to 10.0. High-throughput RNA expression analyses were conducted for both the transcriptome and the miRnome.

### 3.2. Transcriptome based characterization of the MSC identity

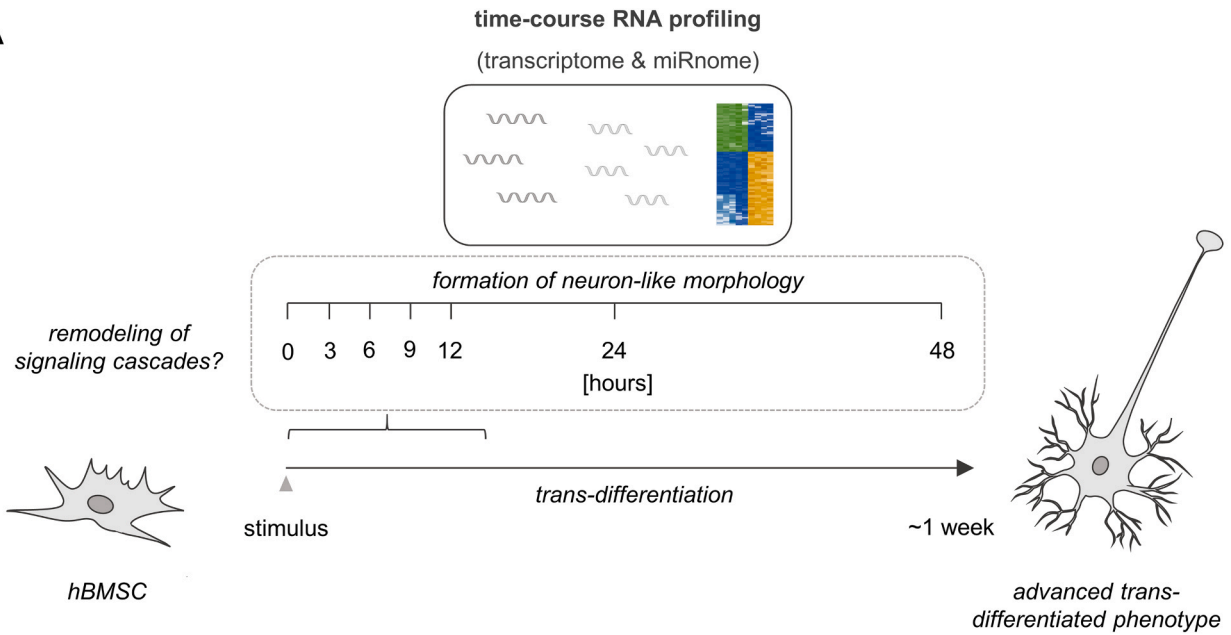
To contribute to a better definition of MSC signatures, we examined the expression of conventional MSC markers and of recently reported gene signatures in the analysis of our transcriptomics data (Fig. 1B and C). We first focused on the time-point before stimulation of the trans-differentiation process i.e., the 0 h time-point of our time-course analyses.

Our data confirmed high mRNA expression levels of the conventional MSC positive markers, *CD90/THY1*, *CD73/NT5E*, and *CD105/ENG*, as defined by the International Society for Cellular Therapy (ISCT) (Dominici et al., 2006). Corresponding median log<sub>2</sub> expression levels at the 0 h time-point ranged between 10.48 and 15.42. Antibody staining had confirmed these markers on the surfaces of 91 % of the cells (data provided by the PromoCell GmbH, Heidelberg, Germany).

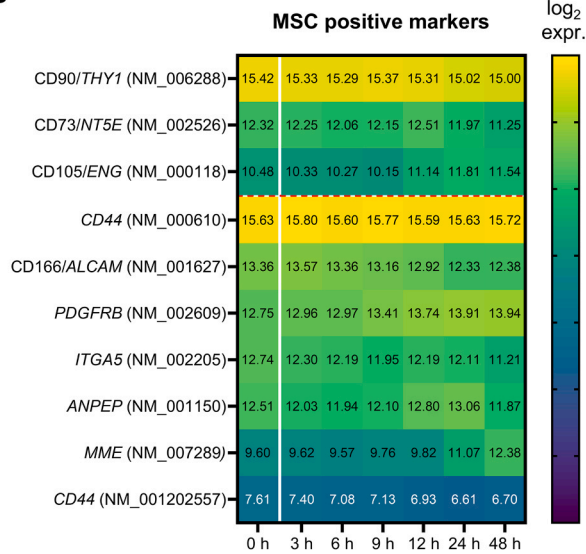
Based on the definition by the ISCT, absence of *CD11B* or *CD14*, *CD19* or *CD79A*, *CD34*, *CD45*, and *HLA-DR* surface molecules is also characteristic for the MSC identity (Dominici et al., 2006). Accordingly, we found comparatively low RNA expression levels of *CD11B/ITGAM* (median log<sub>2</sub> expression: 5.13), *CD14* (median log<sub>2</sub> expression: 6.57), *CD19* (median log<sub>2</sub> expression: 4.27), *CD34* (median log<sub>2</sub> expression: 4.02) and *CD45/PTPRC* (median log<sub>2</sub> expression: 4.74). We found high mRNA expression for *CD79A* with a median log<sub>2</sub> expression of 11.30. We detected comparatively low expression levels of most *HLA-DR* subtypes. The detected *HLA-DRA*, *HLA-DRB4*, *HLA-DRB5* transcripts showed a median log<sub>2</sub> expression of 4.02, 3.91 and 3.27, respectively. *HLA-DRB3* was not detected by our RNA expression analyses. Two mRNA isoforms of *HLA-DRB1* (NM\_002124, NM\_001359194), however, were found with high mRNA expression levels and median log<sub>2</sub> expressions of 7.45 and 8.54, respectively. As for the negative MSC markers *CD14*, *CD34*, *CD45* *CD19* and *HLA-DR*, protein expression was only found on the surfaces of 2–8 % of the cells (data provided by PromoCell).

Extending our MSC marker analysis to other recently suggested signature genes (Rohart et al., 2016), we confirmed high mRNA expression of *ALCAM/CD166* (median log<sub>2</sub> expression: 13.36), *ANPEP* (median log<sub>2</sub> expression: 12.51), *CD44* (median log<sub>2</sub> expression NM\_001202557: 7.61; NM\_001202557: 15.63), *ITGA5* (median log<sub>2</sub> expression: 12.74), *MME* (median log<sub>2</sub> expression: 9.60) and *PDGFRB* (median log<sub>2</sub> expression: 12.75). We detected comparatively low mRNA

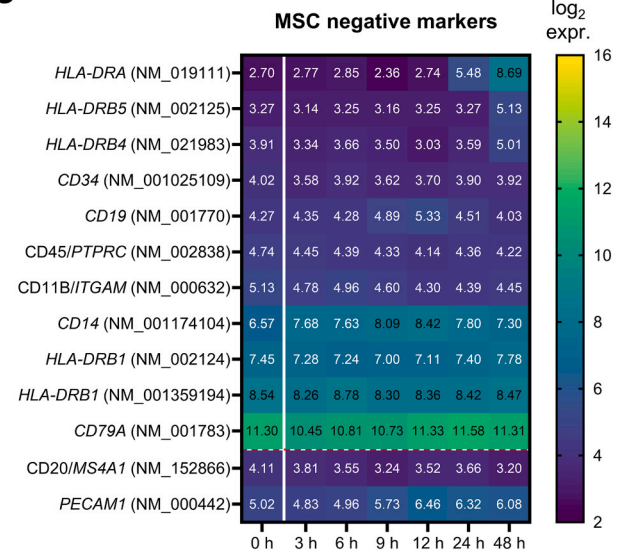
**A**



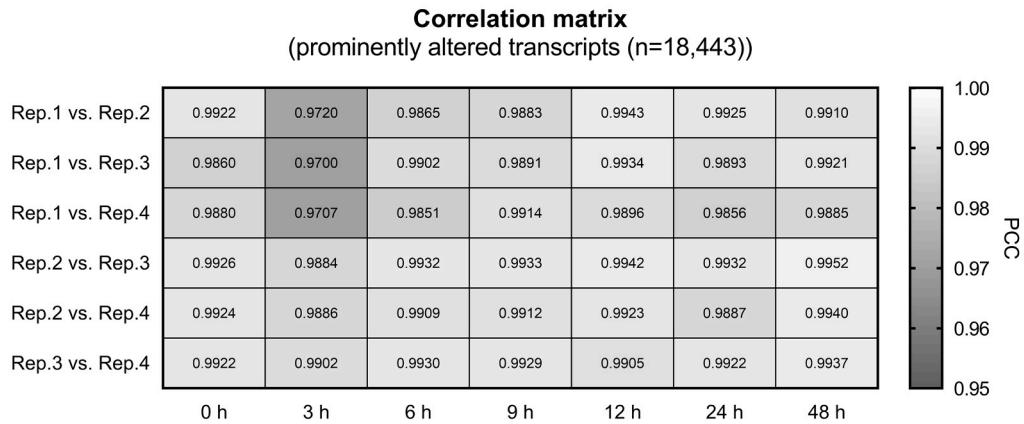
**B**



**C**



**D**



(caption on next page)

**Fig. 1.** Overview of the experimental design, evaluation of MSC identity markers and time-course correlation of prominently altered transcripts. **A:** Trans-differentiation was *in vitro* stimulated by neurogenic differentiation medium to human BMSCs that were grown on the surface of fibronectin coated flasks. Cell samples for subsequent high-throughput mRNA and miRNA expression analyses were collected at early time-points (0, 3, 6, 9, 12, 24 and 48 h) after induction of the trans-differentiation process. The experiment was repeated in four replicates, resulting in a total of 28 RNA time-course samples. **B, C:** The time-course RNA signatures of MSC positive (B) and negative markers (C). Median  $\log_2$  time-course expression patterns are shown for established and recently introduced MSC identity markers, respectively. Separation between these groups is indicated by the red dashed horizontal line. **D:** Expression data of 18,443 transcripts with prominent time-course alterations were compared between the four replicated (rep.) experiments. Resulting Pearson's correlation coefficients (PCCs) are summarized in a correlation matrix.

expression levels of the recently reported negative markers (Oguma et al., 2022; Rohart et al., 2016) *CD20/MS4A1* and *PECAM1* (median  $\log_2$  expression: 5.02).

### 3.3. Overall time-course expression changes

Extending our evaluation to further time-points of the early trans-differentiation process, a change in mRNA expression was evident for most of the MSC marker genes. Compared to the 0 h time-point, declining and increasing expression patterns were detectable in both, the groups of positive and the negative markers. The overall largest expression changes were observed at the end of the time-course analysis, i.e., at the 48 h time-point.

Specifically, out of the positive markers (Fig. 1B), six transcripts showed a declining expression pattern towards the end of the time-course (*CD73/NT5E*, *CD90/THY1*, *ANPEP*, *CD44* (NM\_001202557), *CD166/ALCAM*, *ITGA5*), while three showed an increasing expression pattern (*CD105/ENG*, *MME*, *PDGFRB*) and one transcript remained rather constant (*CD44* (NM\_000610)). The largest time-course expression changes were observed for *ITGA5* and *MME*. Compared to the beginning of the time-course, median  $\log_2$  fold changes ( $\log_2$  FCs) of the corresponding mRNA transcripts were  $-1.53$  and  $2.78$ , respectively.

Out of the MSC negative markers (Fig. 1C), six transcripts showed an increasing expression pattern (*CD14*, *HLA-DRA*, *HLA-DRB1* (NM\_002124), *HLA-DRB4*, *HLA-DRB5*, *PECAM1*), four showed a declining expression pattern towards the end of the time-course (*CD11B/ITGAM*, *CD19*, *CD45/PTPRC*, *CD20/MS4A1*) and three remained rather constant as compared to the beginning (*HLA-DRB1* (NM\_001359194), *CD34*, *CD79A*). Here, the largest time-course expression changes were observed for *CD20/MS4A1* and *HLA-DRA* with median  $\log_2$  FCs of the corresponding mRNA transcripts at  $-0.92$  and  $5.99$ , respectively.

### 3.4. Grouping of transcripts in the early trans-differentiation process

We next identified transcripts with the most prominent time-course alterations and evaluated their functional relations. For each of the 35,369 detected transcripts, the maximum and minimum expression levels throughout the time-course were determined based on the median results of four independent time-course experiments. Comparing the corresponding time-points, prominent expression changes were defined by a median fold change (FC) criterion of  $\geq 1.5$  and their statistical significance ( $p \leq 0.05$ ) after False Discovery Rate (FDR) correction. We identified 18,443 transcripts with prominent time-course alterations, comprising 9,009 transcripts with an overall decreased expression and 9,434 transcripts with an overall increased expression over the 48-hour time-period.

Comparing the expression data of the transcripts with prominent alterations revealed a very high concordance between the four replicated time-course experiments (Fig. 1D), demonstrating a rather uniform progress of the trans-differentiation process. For most of the comparisons the correlation coefficients were above a level of 0.985. A slightly reduced correlation was only observed for replicate 1 at the 3 h time-point, likely indicating some technical issues as compared to the other time-course replicates. However, corresponding Pearson's correlation coefficients were still in a high range between 0.970 and 0.972. This consistency allowed grouping the prominently altered transcripts

into distinct clusters, each with a specific expression pattern over the time-course.

### 3.5. Cellular processes associated with transcript clusters

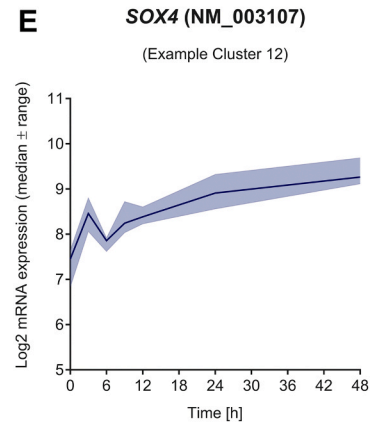
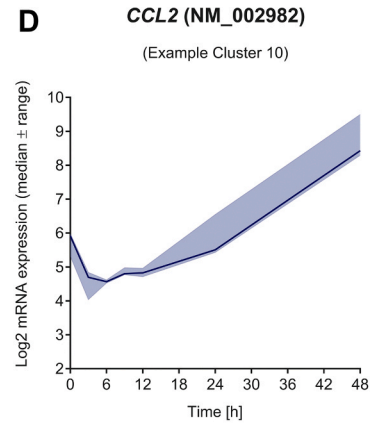
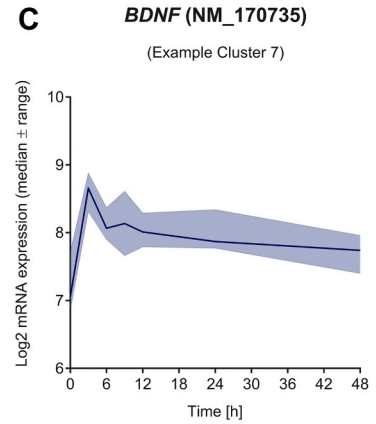
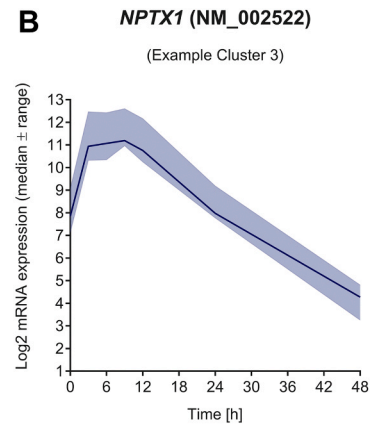
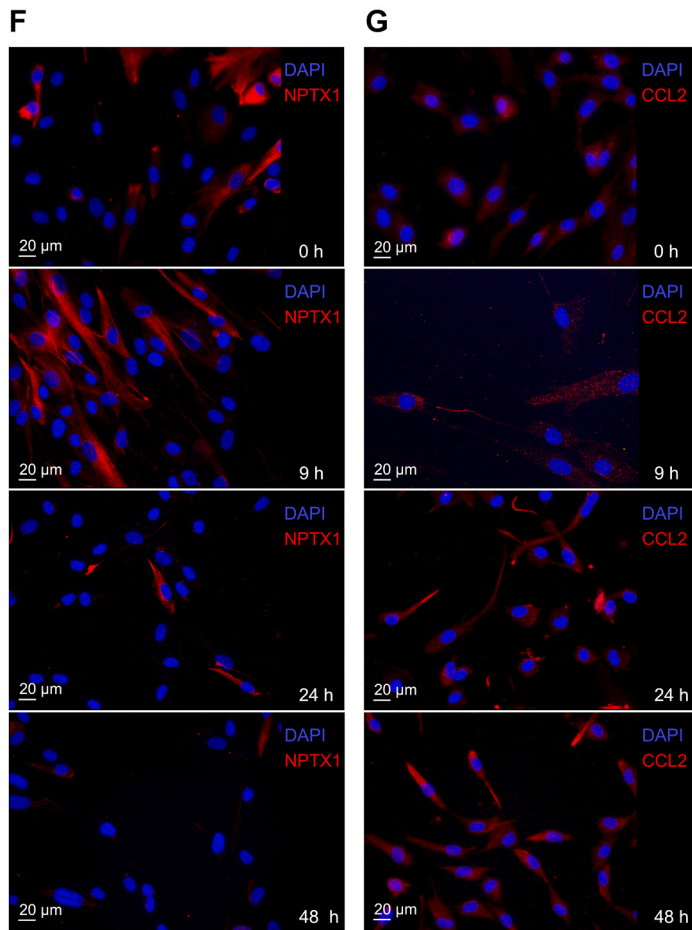
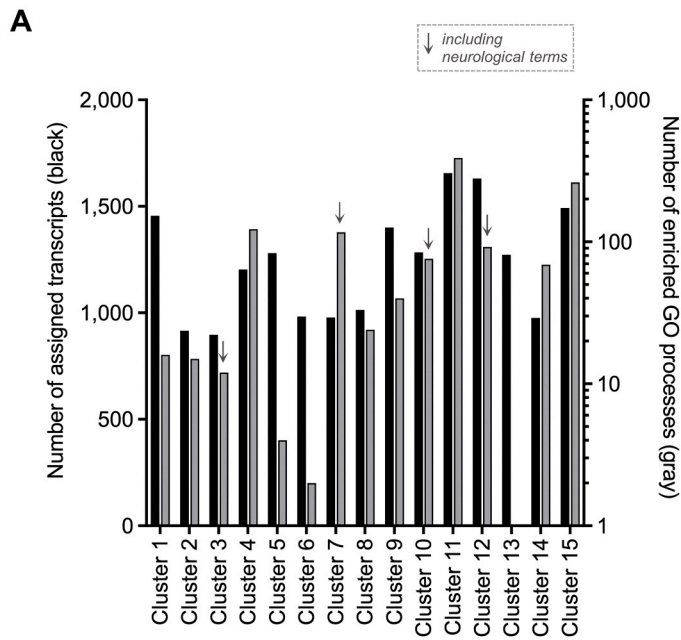
Categorization of the overall 18,443 prominently altered transcripts, identified 15 distinct clusters of expression trajectories (Supplementary Figure S1). Cluster 11 encompassed the highest number of transcripts, with a total of 1,656, while cluster 3 represented the smallest group with 897 transcripts (Fig. 2A left axis). To facilitate a comprehensive overview, the transcriptome and clustering data have been compiled in an atlas format and appended to the supplementary materials (Supplementary Table S1).

To unveil functional associations with cellular processes, enrichment analyses for each of the clusters were performed using the STRING 11.5 *in silico* tool (Szklarczyk et al., 2021). Considering "GO (Gene Ontology) biological processes" (Harris et al., 2004), the most significant terms were attributed to cluster 11 ( $n=390$ ), whereas no significant relations to specific cellular processes were identified for Cluster 6. Supplementary table S2 summarizes the top 20 enriched GO processes for each cluster based on p-values (see also Supplementary table S3). Corresponding functional associations can be assigned to various head categories, including "cellular adhesion", "ribosome production and function", "transferRNA production and function", "mitosis and replication", "immune system and interferone signaling", "transcriptional activity", "metabolism", and "development and differentiation".

Upon searching for the terms "neuron" and "nervous" among the significantly enriched processes, specific functions were identified for four out of the 15 clusters, including the clusters 3, 7, 10, and 12 (Fig. 2A right axis). The expression trajectory of cluster 3, exemplified by the *NPTX1* transcript, showed an early increase followed by a plateau-like phase and a sharp decrease for the remaining time-points (Fig. 2B). Cluster 7, represented by the *BDNF* transcript, exhibited an early increase followed by a very slight decrease at later time points (Fig. 2C). The expression trajectory of cluster 10, as represented by the *CCL2* transcript, displayed an early decrease followed by a sharp increase for the remaining time points (Fig. 2D). Cluster 12, exemplified by the *SOX4* transcript, represented a sharp increase, followed by a short decrease and a steady increase during the time course (Fig. 2E).

Besides the enriched GO processes, we identified enrichment of various "Monarch human Phenotype Ontology" (Monarch HPO) (Shefchek et al., 2020) terms denoting specific relations to neurological abnormality and Central Nervous System (CNS)-associated diseases (Supplementary Table S3). These terms were significantly enriched in clusters 12 and 15. Among the genes in cluster 12 that were associated with "Abnormality of the nervous system (HP:0000707)" (adj.  $p=5.60 \times 10^{-3}$ ;  $n=248$ ) were for example *CYP11B1*, *MGP*, and *NTN1*. Among the genes in cluster 15 that were associated with "Neurodevelopmental abnormality (HP:0012759)" (adj.  $p=1.02 \times 10^{-2}$ ;  $n=160$ ) were for example *NEK2*, *BLM*, and *NALCN*.

Next, we exemplarily show protein expression of the neuronal pentraxin 1 (NPTX1/NP-I) and C-C motif chemokine ligand 2 (CCL2/MCP1) during 48 h of trans-differentiation. For each time-point and each protein, expression was analyzed in 100 cells. Our cellular protein staining shows moderate fluorescence intensities of NPTX1 in about 25 % of the MSCs prior to the differentiation (Fig. 2F). After 9 h of trans-differentiation, the cells exhibited strong fluorescence intensities with



(caption on next page)

**Fig. 2.** Representation of prominently altered transcripts by 15 clusters of time-course expression trajectories. A: For the 18,443 prominently altered transcripts different shapes of expression trajectories are represented by 15 distinct clusters. The numbers of transcripts that have been assigned to each of the clusters are indicated by the black bars and the scale on the left axis. The numbers of significantly enriched Gene Ontology (GO) cellular processes per cluster are indicated by the gray bars and the scale on the right axis of the graph. Clusters that include functional connections to neurological processes are marked with arrows. B-E: Expression trajectories of the clusters that were enriched for neurological terms are exemplarily represented by *NPTX1*, *BDNF*, *CCL2* and *SOX4*. Log<sub>2</sub> expression data are shown as median results (line) with total ranges (filled areas) of the four replicated time-course experiments. F, G: Selected time-course expression patterns were confirmed by fluorescence microscopic analysis of neuronal pentraxin 1 (NPTX1) and C-C motif chemokine ligand 2 (CCL2) proteins. Characteristic time-points were chosen based on the corresponding time-course RNA expression data (see B, D). Representative fluorescence microscopic images were taken at a resolution of 40x. DAPI staining of cellular nuclei is depicted in blue and immune fluorescence staining of NPTX2 (F) or CCL2 (G) proteins is depicted in red, respectively.

a strong staining of cellular extensions. After 24 h and 48 h of trans-differentiation only about 8 % and 0.5 % of the cells, respectively, showed NPTX1 immune fluorescence. Protein expression analysis of CCL2 expression (Fig. 2G) showed weak fluorescence staining all cells at the 0 h time-point. After 9 h of trans-differentiation, almost 50 % of cells exhibited CCL2 immune fluorescence, albeit at low intensities. After 24 h and 48 h of trans-differentiation 75 % and 90 % of cells, respectively, showed enhanced CCL2 fluorescence staining. Overall, our immune fluorescence analyses are consistent with the expression changes observed by the RNA time-course analyses.

### 3.6. Cellular processes associated with most altered transcripts

In-depth examination of the top 100 transcripts with the most outstanding fold changes revealed high time-course correlations (Fig. 3A and B). For the specific comparisons, most correlation coefficients were above 0.94. Slightly reduced correlations were only observed for replicate 1 at the 3 h time-point, ranging between 0.858 and 0.890 for the top 100 decreasing and between 0.878 and 0.904 for the top 100 increasing transcripts, respectively.

An analysis of the top 100 decreasing transcripts revealed functional associations (Fig. 3C), such as with p53 signaling, including genes like *GTSE1*, *RRM2*, and *CCNE2*, and with cell cycle regulation, including *CDC45* and *MCM5*. Others of the most decreasing transcripts were linked to the maintenance of stemness, including *BIRC5*, *HMMR*, and *MYB*.

For the top 100 transcripts with increasing expressions (Fig. 3D), functional associations with prostaglandin signaling were evident, including genes such as *CHI3L1*, *PTGDS* and *PPARGC1A*. In addition, among the top transcripts with increasing expression were genes involved in complement signaling, including *C5AR1*, *CDKN1C* (p57) and *C1S/C1R* and genes involved in extracellular matrix remodeling, such as *MMP13*, *EFEMP1* and *FMOD*.

### 3.7. Time course expression of marker genes characteristic for the neural lineage differentiation and synapse maturation

To further depict the specificity of the MSC neurogenic trans-differentiation process, we evaluated the expression of characteristic marker genes for the neural lineage differentiation in context with our time-course experiments.

From the beginning of the time-course, high mRNA expression of the NSC marker nestin (*NES*) (median log<sub>2</sub> expression at 0 h: 10.78) indicated the neural differentiation capability of the analyzed MSCs (Minguell et al., 2005) (Fig. 4A). Likewise, high transcript levels of *MSI1* (median log<sub>2</sub> expression: 8.23) and *VIM* (median log<sub>2</sub> expression: 17.45) were observed at the 0 h time-point. Notably, the mRNAs of all the three NSC markers (Oikari et al., 2016a; Sun et al., 2008) showed rather constant decreases towards the end of the time-course, but still remained at high levels at the 48 h time-point (*NES*: 9.76; *MSI1*: 7.39; *VIM*: 17.18). For *NES* and *MSI1* these prominent decreases were statistically significant.

We next characterized the RNA expression of common neuron differentiation markers (Coccini et al., 2023; Fan et al., 2020; Jandial et al., 2008; McKenzie et al., 2018; Oikari et al., 2016a, 2016b; Shi et al., 2018; Sun et al., 2008) in context with our BMSC time-courses experiments

(Fig. 4B).

Amongst the neuron markers with the highest overall expression, *TUBB3* and *ENO1* showed distinct transcript expression already at the 0 h time-point, i.e. before stimulation of the trans-differentiation process (median log<sub>2</sub> expression *TUBB3* (NM\_006086): 15.28; *ENO1* (NM\_001428): 15.13). It is known that *TUBB3* is expressed in mesenchymal as well as neural lineages (Tondreau et al., 2004). With time progression a minor decline of the corresponding mRNAs was observed. Compared to the time-points of maximal and minimal expression, ten out of the overall 22 marker transcripts, displayed prominent time-course increases (*BTBD11* (NM\_001018072), *DISP2* (NM\_033510), *GAP43* (NM\_002045), *MAPT* (NM\_001123066), *MAPT* (NM\_016835), *NEFM* (NM\_005382), *RBFOX3* (NM\_001350453), *SCN2A* (NM\_021007), *SYT13* (NM\_020826), *ZMAT4* (NM\_024645)) and were, thus, listed in the atlas of Supplementary Table S1. Vice versa, six of the marker transcripts displayed prominent time-course decreases (*DLX2* (NM\_004405), *ENO1* (NM\_001428), *ENO2* (NM\_001975), *GAD1* (NM\_013445), *SERTM1* (NM\_203451), *SYN1* (NM\_006950)).

In addition to general neuron markers, we also characterized the expression patterns of common markers for synapse maturation (Cline, 2005; Coccini et al., 2023; Elias et al., 2008; Gomez de San Jose et al., 2022; Krueger et al., 2012; Kwon and Chapman, 2011; Pelkey et al., 2015; Varoqueaux et al., 2006) (Fig. 4C). Out of the 13 analyzed marker transcripts, six displayed a prominent increase in expression during the time-course (*DLG4* (NM\_001365), *NLGN2* (NM\_020795), *NLGN4X* (NM\_001282145), *NPTXR* (NM\_014293), *NRXN2* (NM\_138732), *SYP* (NM\_003179)). For example, *NLGN2* (NM\_020795) continuously increased from a value of 9.60–11.93 during the initial 12 h of trans-differentiation. Afterwards the expression increase leveled off, reaching a maximum of 12.04 after 24 h, and ended with a final level of 11.71 (48 h). Another isoform of *NLGN2* (ENST00000575301) represented the transcript with the overall highest expression level and showed only minor changes with a short-term decrease from 12.92 to 12.14 at the 3 h time-point. Two synapse maturation markers showed prominent time-course decreases (*NPTX1* (NM\_002522); *NPTX2* (NM\_002523)). As described above and shown in Fig. 4C, the *NPTX1* transcript displayed a remarkable increase during the early 12 h of trans-differentiation (median log<sub>2</sub> expression *NPTX1* (NM\_002522) 0 h: 7.85; 12 h: 11.19). With time progression, inversion of this trend towards an overall decline could be observed, resulting in a final median log<sub>2</sub> expression level of 4.27.

We exemplarily evaluated the time-course protein detection of nestin (*NES*) and  $\beta$ -tubulin III (*TUBB3*) in 100 cells (Fig. 4D-G and Supplementary Fig. S2 A-D). At the beginning of the time course (0 h) nestin expression was detected in 50 % of the cells and decreased remarkably until 48 h with only few cells with nestin expression at the ends of cell extensions. In contrast  $\beta$ -tubulin III expression at the beginning (0 h) was detectable in almost all cells. During the following 48 h  $\beta$ -tubulin III expression was detectable in 95 % of cells with strong expression in whole cell bodies and extensions. To allow for further assessment, we extended our observations of *NES* and *TUBB3* proteins to the advanced stages of the trans-differentiation (Fig. 4H and I and Supplementary Fig. S2E and F). Interestingly after 3 days cells with simultaneous nestin and  $\beta$ -tubulin III expression in dendrites were detected and after 7 days nestin expression increased predominantly at the ends of dendrites, while  $\beta$ -tubulin III expression decreased at the ends of those.

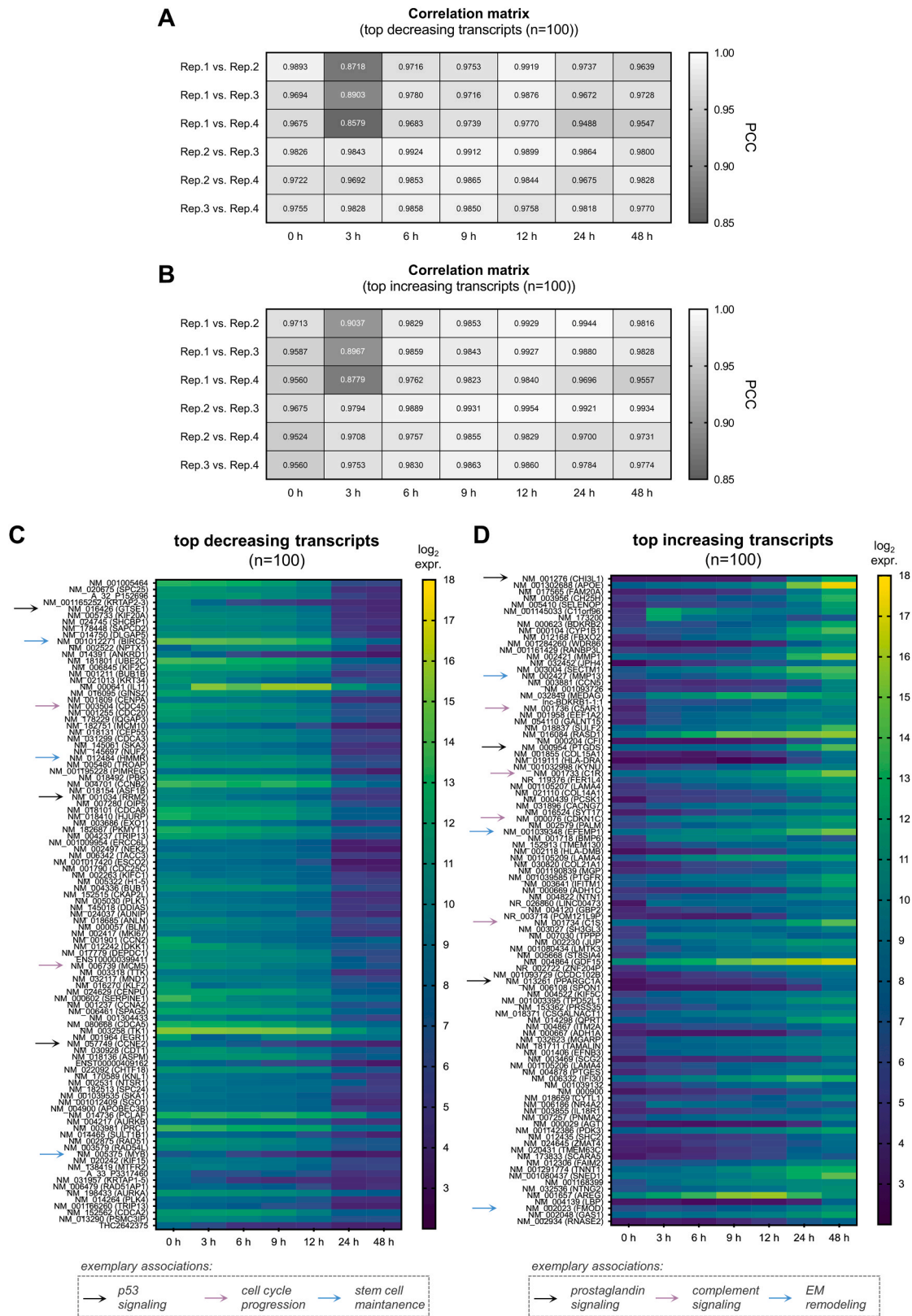


**Fig. 3.** Overview on the top hundreds of prominently altered RNA transcripts. A, B: Amongst the 18,443 prominently altered transcripts, the 100 with the highest fold changes were determined and separated according to decreasing (A) and increasing (B) expression levels. Corresponding expression data were compared between the four replicated (repl.) experiments. Resulting PCCs are summarized in the correlation matrices. C, D: The top 100 transcripts are listed and represented with their median  $\log_2$  time-course expression. For the top 100 decreasing transcripts (C) associations with the p53 signaling, cell cycle progression and stem cell maintenance are marked by differently colored arrows as specified in the image. For the top 100 increasing transcripts (D) examples with functional associations to prostaglandin signaling, complement signaling and extracellular matrix remodeling are marked accordingly.

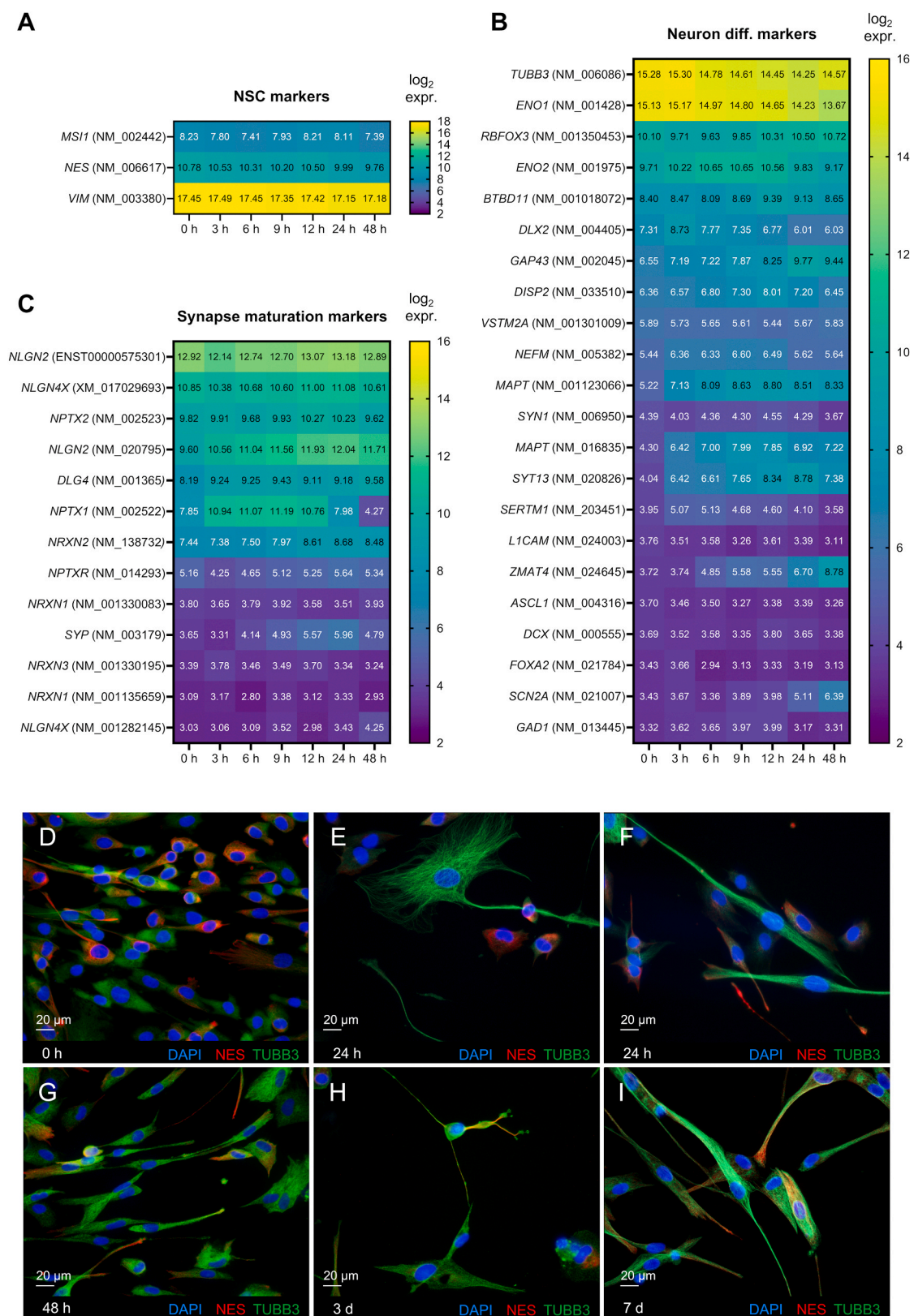


**Fig. 4.** Time-course evaluation of neural stem cell (NSC), neuron differentiation and synapse maturation markers. A-C: Time-course RNA expression data were evaluated for markers of common neural stem cells (NSC), neuron differentiation (diff.) and synapse maturation markers. Log<sub>2</sub> expression patterns of the corresponding transcripts are shown as median results of the four time-course experiments. D-I: Selected time-course expression patterns were confirmed by fluorescence microscopic analysis of nestin (NES) and class III  $\beta$ -tubulin (TUBB3) protein expression. Protein analyses were conducted at selected time-points during the early trans-differentiation process (0, 24 and 48 h; D-G) and after an extended period of 3 days (H) and 7 days (I), respectively. We show two exemplary pictures of the 24 h time-point to emphasize the early structural alteration and  $\beta$ -tubulin III expression within the cells. Representative fluorescence microscopic images were taken at a resolution of 40x. DAPI staining of cellular nuclei is depicted in blue. Immune fluorescence staining of NES and TUBB3 is depicted in red and green, respectively.

### 3.8. Time-course expression of astrocyte and oligodendrocyte markers

We further extended the evaluation of our hMSC time-courses data to various astrocyte (Fan et al., 2020; Jandial et al., 2008; McKenzie et al., 2018; Oikari et al., 2016b; Spurgat and Tang, 2022; Zhang et al., 2019) and oligodendrocyte differentiation markers (Huang et al., 2020; Jandial et al., 2008; Li et al., 2017; McKenzie et al., 2018; Oikari et al., 2016b; Zheng et al., 2018).

Nine out of the overall 18 astrocyte marker transcripts (Fig. 5A) displayed prominent time-course increases as specified above (*CLDN10* (NM\_182848), *HES1* (NM\_005524), *PRSS35* (NM\_153362), *S100B* (NM\_006272), *SLC1A2* (NM\_004171), *STAT3* (NM\_213662), *TPD52L1* (NM\_001003395), *TPD52L1* (NM\_001292026), *NDRG2* (NM\_001354565)). A distinct time-course increase was observed for example for *PRSS35* (NM\_153362). Starting at a median  $\log_2$  expression value of 4.23, the expression quickly raised, but flattened towards the end of the time-course, resulting in final level of 9.65. Three of the astrocyte marker transcripts displayed prominent time-course decreases (*ALDH1L1* (NM\_012190), *CD44* (NM\_001202557), *ID1* (NM\_002165)). For example, the *CD44* marker (NM\_001202557), showed an initial median  $\log_2$  expression of 7.61 (0 h) decreasing to a level of 6.70 (48 h). Another isoform of the *CD44* marker (NM\_000610) represented the astrocyte marker with the overall highest expression level and showed a rather constant expression trajectory during the time-course, ranging between 15.59 and 15.80.

Amongst the oligodendrocyte differentiation markers (Fig. 5B), *PDGFRA* showed the overall highest expression starting with a median  $\log_2$  expression of 11.56 (0 h) and displaying a minor increase to a level

of 14.61 (48 h). *PDGFRA* is involved in the growth and migration of mesenchymal cells as well as the signaling of oligodendrocyte progenitors (Funa and Sasahara, 2014). Six out of the overall 15 marker transcripts displayed prominent time-course increases as specified above (*CARNS1* (NM\_001166222), *EGFR* (NM\_201283), *PAIP2B* (NM\_020459), *PDGFRA* (NM\_006206), *QDPR* (NM\_000320), *TMEM144* (NM\_018342)). A remarkable increase in mRNA expression was observed, for example, for *TMEM144* (NM\_018342), starting from a median  $\log_2$  expression of 6.32 (0 h) and reaching a level of up to 7.94 (48 h). Four of the oligodendrocyte marker transcripts displayed prominent time-course decreases (*ANLN* (NM\_018685), *CSPG4* (NM\_001897), *EGFR* (NM\_005228), *GALC* (ENST00000622264)). The *ANLN* (NM\_018685) transcript, for example, showed a continuous mRNA decrease from a median  $\log_2$  expression of 11.18 (0 h) to 6.12 (48 h) during the time-course.

### 3.9. Validation of time-resolved RNA expression patterns

Further validation of the microarray results was performed using RT-qPCR. *ITGA5* was chosen as a marker for MSC identity, *MMP13* as one of the top transcripts with increased expression, *NES* as a marker for NSCs, and *NLGN2* and *NPTX1* as markers for synapse maturation. Additionally, *TUBB3* and *GAP43* were analyzed as markers for neuronal differentiation, while the time-course mRNA expression patterns of *ANLN* and *PRSS35* were validated as markers for oligodendrocyte and astrocyte differentiation, respectively.

Re-analyzing our time-course RNA samples by an independent method, we found a striking similarity between the results of the RT-

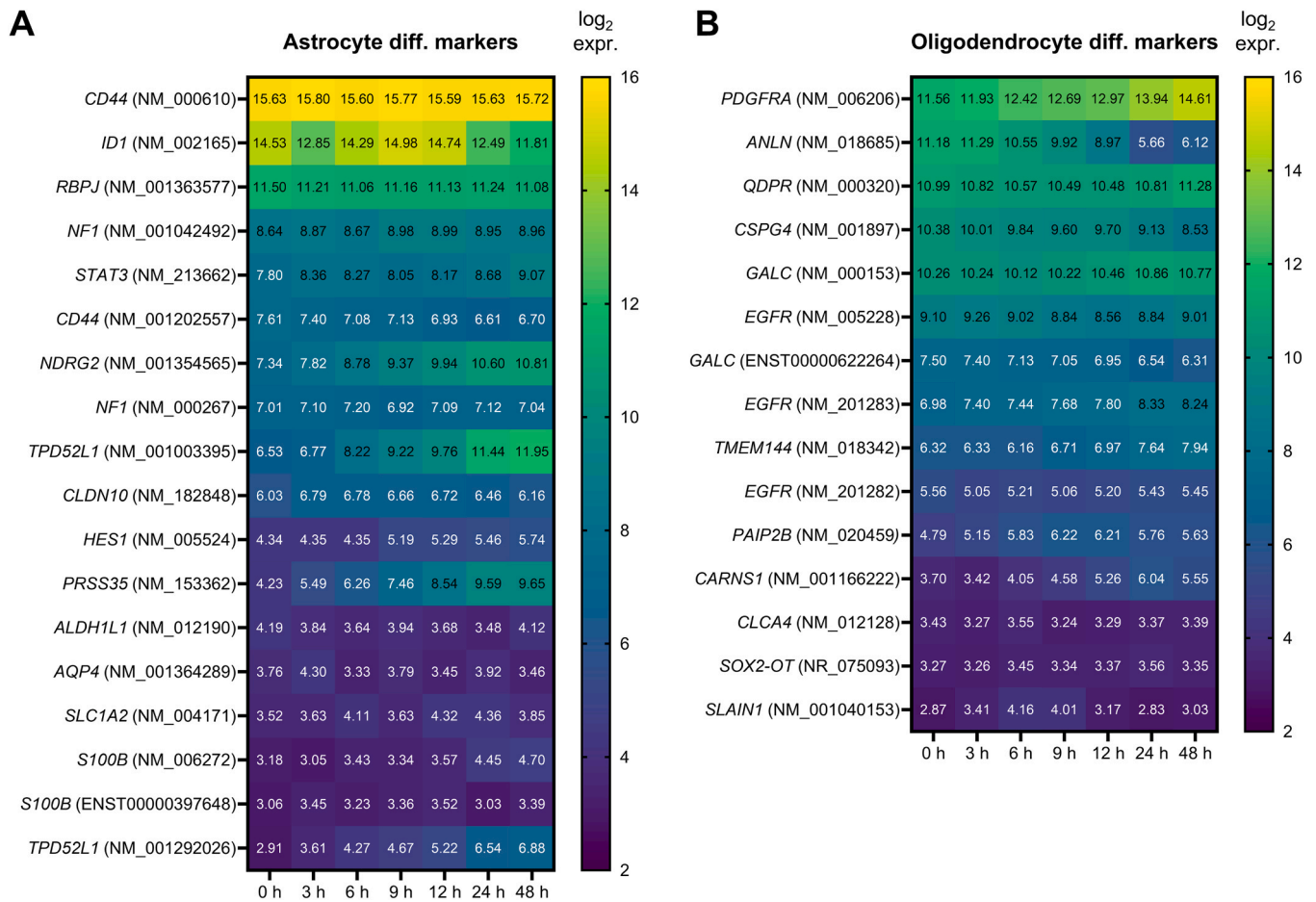


**Fig. 5.** Time-course evaluation of oligodendrocyte and astrocyte differentiation markers. Time-course RNA expression data were evaluated for common astrocyte (A) and oligodendrocyte (B) differentiation (diff.) markers.  $\log_2$  expression patterns of the corresponding transcripts are shown as median results of the four time-course experiments.

qPCRs and the median results of the original microarray analyses. As shown in Fig. 6, the comparative analysis confirmed that both the ranges and shapes of the time-course patterns matched, confirming the validity of our microarray data.

As determined by RT-qPCR analyses, marker expression was different between trans-differentiated cells and control cells with mesenchymal maintenance medium as exemplified for expression of neuron differentiation marker *GAP43* and synapse maturation marker *NLGN2* and MSC marker *ITGA5* (Supplementary Fig. S3).

### 3.10. Time-course expression of microRNAs in the early trans-differentiation process

MicroRNAs (miRNAs) exhibit their function by inducing expression reduction of their specific target genes at the post-transcriptional level (Bartoszewski and Sikorski, 2018; Diener et al., 2023b; Yao, 2016). To investigate the potential impact of miRNA-mediated post-transcriptional regulation as part of the trans-differentiation process, we conducted a comprehensive analysis of the miRNome alongside the transcriptome at time-points 0, 3, 6, 9, 12, 24, and 48 h, following trans-differentiation induction.

We identified 91 prominently altered miRNAs exhibiting significant time-course expression changes with a fold change  $\geq 1.5$ . Among them, 46 demonstrated an overall decreased expression, while 45 displayed increased expression over the 48-hour period.

As for the mRNA transcripts we examined the dynamics of changes in the median  $\log_2$  miRNA expression over the 48-hour timespan. High time-course consistency between the replicated experiments, comprising correlation coefficients of more than 0.960 (Supplementary Figure S4A), allowed grouping of the 91 prominently altered microRNAs into distinct clusters, each representing a specific expression pattern over the time-course. The various expression trajectories were categorized into five distinct clusters (Supplementary Fig. S4B). As for the transcriptome data, the miRNome expression and clustering data are provided in an atlas format in the supplementary materials (Supplementary Table S4).

Cluster 2 contained the highest number of miRNAs, with a total of 33, while clusters 4 and 5 were the smallest with 12 miRNAs each (Fig. 7A). Cluster 1, typified by a continuous decrease in expression following an initial latency of approximately 12 h, was exemplified by hsa-miR-15b-5p (Fig. 7B). Cluster 2, characterized by a continuous increase in expression after a certain latency period of 6 h, was exemplified by hsa-miR-27b-3p (Fig. 7C). Cluster 3, displaying a continuously decreasing expression trajectory, included several members of the miR-17 family, such as hsa-miR-18a-5p (Fig. 7D). Cluster 4 with a continuously increasing expression trajectory, encompassed various members of the let-7 miRNAs, including hsa-let-7c-5p (Fig. 7E). Cluster 5 was marked by an early decrease followed by a plateau-like phase at later time-points, featured 12 miRNAs including hsa-miR-503-5p (Fig. 7F).

To quantify the above-described expression changes, we utilized a calibration curve from a previous study (Diener et al., 2020), revealing that the most prominent alterations ranged within a magnitude of  $10^2$ - $10^3$  molecules per cell during the 48-hour observation window. Notably, this range aligns well with findings in other cell types (Diener et al., 2020). Among the top miRNAs with the largest changes in molecular expression were for example hsa-let-7b-5p with +4,103 molecules/cell, hsa-miR-6089 with +2,311 molecules/cell, hsa-miR-34a-5p with +1,577 molecules/cell, hsa-miR-1260b with -2,303 molecules/cell, hsa-miR-221-3p with -520 molecules/cell and hsa-miR-15b-5p with -335 molecules/cell (Fig. 7G).

To gain insight into the regulatory roles of the prominently altered miRNAs, we searched for experimentally validated miRNA-target interactions using the *in-silico* tool miRTargetLink 2.0 (<https://ccb-compute.cs.uni-saarland.de/mirtargetlink2>) (Kern et al., 2021a). Since miRNAs often exert their regulatory effects by causing a decrease in the expression of their mRNA targets (Guo et al., 2010), we utilized the

time-course expression data to identify inversely expressed targets. We identified 203 miRNA-target interactions for the 45 miRNAs with increasing miRNA expression levels and 341 target interactions for the 46 miRNAs with decreasing expressions (see Supplementary Table S5). Subsequently, we constructed interaction networks for the corresponding proteins using the STRING 11.5 database (Szklarczyk et al., 2021) and highlighted sub-networks associated with the GO term "neuron differentiation" (Fig. 8A and B). Within the network for decreasing miRNAs, we identified central nodes such as *STAT3* and *VEGFA* mRNAs, both of which displayed increased expression during the observed time-course (Fig. 8A). The corresponding proteins have previously been linked to neural differentiation and MSC trans-differentiation (Snyder et al., 2011; Theis and Theiss, 2018; Wada et al., 2006). Within the networks for increasing miRNAs, we identified central nodes such as *MAPK1* and *MET*, both of which exhibited decreased expression over the time course (Fig. 8B). The expression of these appears to be restricted to specific stages of the neural differentiation process (Semprich et al., 2022; Zheng et al., 2013).

## 4. Discussion

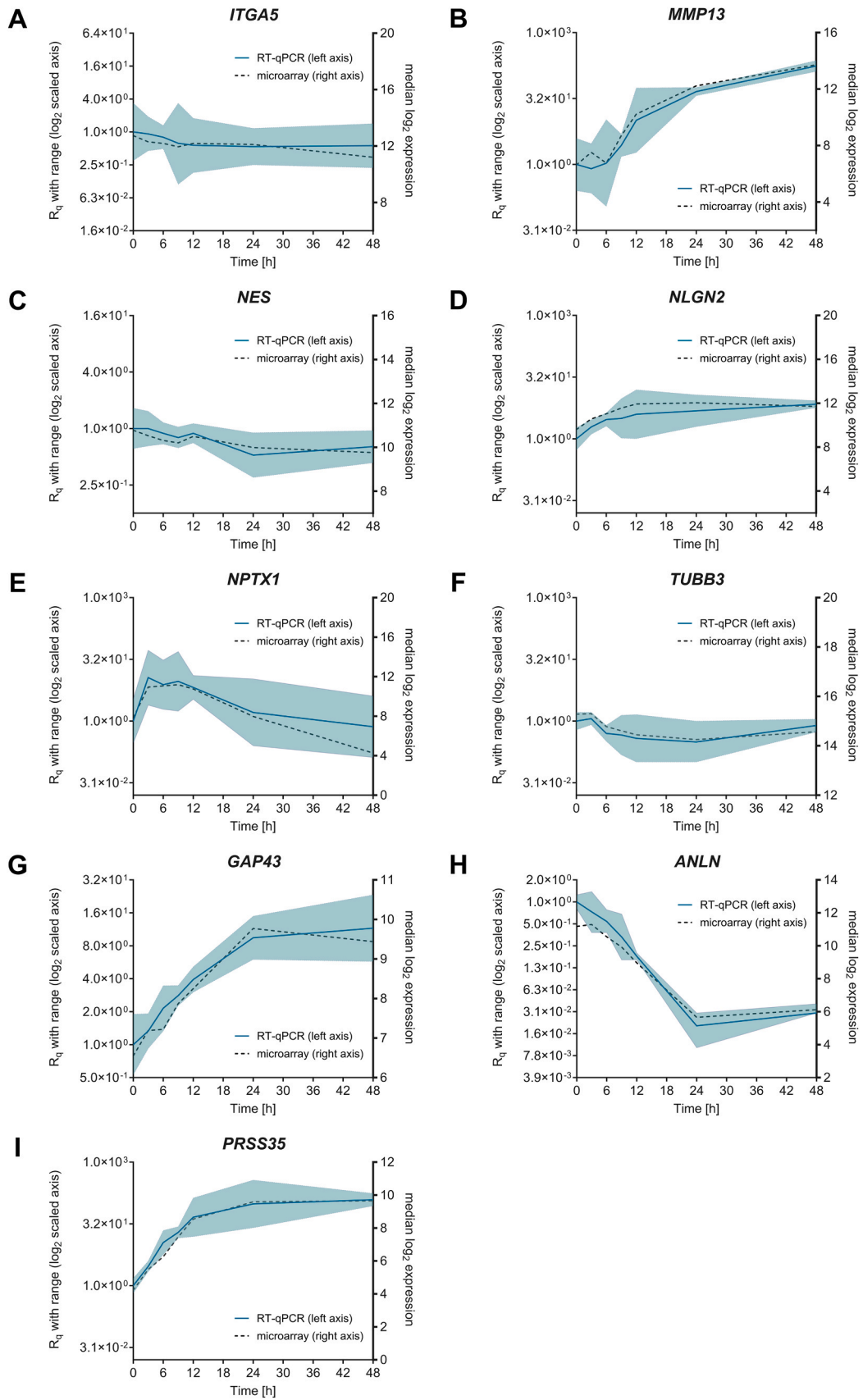
The ISCT defines MSC identity through the expression of specific surface markers (Dominici et al., 2006). However, the definition of clear signatures remains controversial due to heterogeneous results and is an ongoing process (Musial-Wysocka et al., 2019; Pittenger et al., 2019; Wang et al., 2021). Nonetheless, there is growing evidence that gene expression data can refine the criteria for a more precise definition of MSC identity (Pittenger et al., 2019). A major aim of our study was to contribute to this effort by better defining MSC signatures.

Most of the conventional and various recently introduced markers appear to efficiently indicate MSC identity. We found high RNA expression levels of various MSC positive markers including genes such as *CD44*, *THY1* (CD90), *NTSE* (CD73), *ENG* (CD105), *ALCAM* (CD166), *ITGA5*, *MME* and *PDGFRB*. Notably, *CD44* has also been considered as an intermediate marker for astrocyte differentiation from human pluripotent stem cells (Cai et al., 2012; Oikari et al., 2016b; Shaltouki et al., 2013). Low mRNA expression was detected for several MSC negative markers including *ITGAM* (CD11B), *CD14*, *CD19*, *MS4A1* (CD20), *CD34*, *PTPRC* (CD45), *PECAM1* and most *HLA-DR* isoforms. Consistent with our findings of an elevated expression of *HLA-DRB1*, an independent study also detected high *HLA-DRB1* mRNA expression in human BMSCs. The elevated expression was, however, not confirmed at the protein level (Oguma et al., 2022).

Our time-course transcriptomics data identified several markers like *ITGA5* or *HLA-DRA* that showed an altered expression shortly after the cellular stimulation. These markers appear to be well suited to distinguish between the original MSC identity and the emerging neurogenic trans-differentiation.

Our analysis of transcripts with significant time-course alterations aimed to decipher the transcriptional restructuring that drives MSCs towards a neuron-like phenotype (Cortes-Medina et al., 2019; Khan et al., 2020). Our data highlight functional connections to cellular processes, typically involved in neuronal differentiation.

Various transcripts that exhibit substantial decreases over the time-course, have been associated with p53 signaling and cell cycle progression. Exemplary genes, such as *GTSE1*, *RRM2* and *CCNE2*, are regarded as p53 negative regulators (Gorjala et al., 2016; He et al., 2017; Monte et al., 2003; Scolz et al., 2012). Examples involved in cell cycle regulation, particularly in S phase transition, included genes such as *CDC45* and *MCM5* (Chapouton et al., 2010; Huang et al., 2022; Quinn et al., 2001). Generally, an altered p53 activity and a delay in cell cycle have previously been linked to neurogenesis in the CNS (Farioli-Vecchioli and Tirone, 2015; Hardwick et al., 2015; Ruijtenberg and van den Heuvel, 2016; Xiong et al., 2020). Other transcripts displayed substantial increases and play critical roles in prostaglandin D2 (Augustyniak et al., 2017; Sakry et al., 2015; Zhou et al., 2015) and in



(caption on next page)

**Fig. 6.** Validation of time-resolved RNA expression patterns by RT-qPCRs. To confirm the microarray results, exemplary RT-qPCR were conducted to validate the mRNA expression patterns for nine representative genes: (A) *ITGA5* as a representative marker for the MSC identity, (B) *MMP13*, the transcript of which was amongst the top increasing mRNAs, (C) *NES* as NSC marker, (D, E) *NLGN2* and *NPTX1* as markers for synapse maturation, (F, G) *TUBB3* and *GAP43* as neuron differentiation markers, (H) *ANLN* as oligodendrocyte and (I) *PRSS35* as astrocyte differentiation marker. As the results of the RT-qPCR analyses, relative quantitation ( $R_q$ ) of the corresponding mRNAs was conducted in relation to GAPDH housekeeping gene expression.  $R_q$  plots are shown on the left axis as median results (turquoise line) with the total range (turquoise shaded) of three replicated time-course experiments that were assayed in technical duplicates. They are illustrated in comparison to the median microarray results (black dotted line; right axis).

complement pathways (Coulthard et al., 2017; Furutachi et al., 2013; Walsh et al., 2017), both of which have been associated with neurogenic differentiation (Coulthard et al., 2017; Nango et al., 2020; Thomas et al., 2000). Notably, similar changes in both prostaglandin and complement signaling were also prevalent during the neurogenic differentiation of human induced pluripotent stem cells (iPSCs) (Augustyniak et al., 2017; Walsh et al., 2017), another type of stem cell with therapeutic potential that can be generated by the reprogramming of somatic cells (Thanaskody et al., 2022).

Alteration of additional processes with common links to neuronal development were identified as the result of our gene set enrichment analyses, including various head categories such as cellular adhesion (Migliorini et al., 2013), ribosomal and transfer RNA (rRNA, tRNA) functions (Fusco et al., 2021; Ramos and Fu, 2019), cell division (Farioli-Vecchioli and Tirone, 2015; McKinnon, 2013), immune signaling (Filiano et al., 2016; Morimoto and Nakajima, 2019), transcriptional activity (Hamby et al., 2008), and cellular metabolism (Fawal and Davy, 2018).

Additionally, there were expression changes in transcripts that have well-established roles in neural differentiation signaling. Examples include *NPTX1* that showed an early increase followed by a sharp decrease for the remaining time-points of our analysis. The specific expression pattern was also verified when staining the according cellular proteins and likely plays a crucial role in the early growth of synapse-like connections (Gomez de San Jose et al., 2022). Likewise, the expression of the transcription factor *SOX4* that showed an increasing expression in our time course analysis, is thought to be crucial for establishing neuronal identity (Bergsland et al., 2006). *CCL2* that also showed an increasing expression, both at the mRNA and protein levels, has former been demonstrated as a common regulator of neuronal functions (Hong et al., 2015). Moreover, the neurotrophic factor *BDNF* that showed altered expression pattern in our MSC trans-differentiation experiments has been associated with neurogenic differentiation. Evidence for a decisive role of BDNF stems from studies showing that BDNF supplementation enhances the efficiency of human neural precursor cell differentiation (Jiao et al., 2014) and that overexpression of the *BDNF* gene promotes the neurogenic trans-differentiation of rodent BMSCs (Liu et al., 2015).

Overall, the nature of the transcripts that are prominently altered in the first few hours following the induction of the trans-differentiation, clearly demonstrates a wide-ranging reorganization of cellular pathways. The according changes likely are the first essential steps towards for the acquisition of neuron-like features.

In addition to the evaluation of the transcriptomics, our data also imply that miRNAs act as potential drivers of the cellular trans-differentiation. As for the early dynamics of miRNAs during neurogenic MSC trans-differentiation, we found altered expression patterns of multiple miRNAs that have previously been associated with the differentiation of neurons. Specifically, hsa-let-7b-5p and hsa-miR-34a-5p that have been linked to neural stem cell differentiation and mature neuron signaling exhibit significant expression changes (Aranha et al., 2011; Kern et al., 2021b; Zhao et al., 2010). MiR-34a-5p has also been considered a potential driver of BMSC neurogenic trans-differentiation in rodent models (Liu et al., 2011). Hsa-miR-221-3p that showed a strong decreased expression during early BMSC trans-differentiation has been linked to the differentiation of neural crest cells (Greene and Tischler, 1976; Hamada et al., 2012). Its downregulation has also been shown to facilitate BMSC differentiation into osteoblasts (Gan et al.,

2020), suggesting an essential role in BMSC differentiation signaling.

Our clustering analysis identified further miRNAs that have previously been connected to neural development and differentiation. An increasing time-course trajectory was identified, for example, for hsa-miR-27b-3p that is an abundant neuronal miRNA, which negatively regulates pluripotency associated genes (Fuchs et al., 2014; Poon et al., 2016). Other examples include several members of the let-7 family that has been linked to the regulation of neural stem cell proliferation and differentiation (Roush and Slack, 2008; Zhao et al., 2010). The miR-17 family, which showed a decreasing time-course pattern in our experiments was previously found to have a reduced expression during progressive brain development (Mao et al., 2014; Xia et al., 2022). Hsa-miR-15b-5p, considered as a negative regulator of *BDNF*, and hsa-miR-503-5p, which likely inhibits neural lineages, also showed decreasing time-course expression patterns (Boone et al., 2017; He et al., 2021).

To date only a portion of the miRNAs that found their way into databases have been validated for their nature as true miRNAs (Alles et al., 2019; Diener et al., 2023b). Some candidates, particularly those with high miRNA numbers, have only been annotated based on recent RNA sequencing data and may not necessarily represent true miRNAs. However, this does not imply the absence of cellular functions for the corresponding molecules (Diener et al., 2024). Future analyses should explore the potential roles of poorly characterized miRNAs, like hsa-miR-1260b and hsa-miR-6089, which show significant expression changes in our time-course data. Nevertheless, our evaluation of experimentally validated miRNA-target interactions indicated multiple neuronal differentiation genes as potential targets of miRNAs in the context of neurogenic trans-differentiation. The finding of many shared miRNA-targets within the corresponding regulatory networks underscores the functional interaction of different miRNAs to enhance their regulatory efficiency (Bartoszewski and Sikorski, 2018; Diener et al., 2022, 2023b; Gebert and MacRae, 2019; Schmitz et al., 2014; Selbach et al., 2008).

MSCs' ability to trans-differentiate into neural cells makes them a promising source for treating neurological injuries and neurodegenerative diseases. However, given the critical nature of transplanting MSC-derived neurons into the CNS, safety assessments are crucial. Our time-course analyses suggest potential issues with the neural trans-differentiation process that warrant further investigation.

Prominent time-course alterations of several transcripts indicate associations with CNS abnormalities and diseases of the nervous system. Expressional increases of specific transcripts such as *CYP11B1*, *MGP* and *NTN1* (Alsubait et al., 2020; Mertsch et al., 2009; Ylivinkka et al., 2017) have previously been associated with the development of brain resident tumor entities. In addition, a reduced expression of *BLM* has been associated with genomic instability and a high predisposition to tumors (Cunniff et al., 2017; van Wietmarschen et al., 2018), while substantial reduction of *NALCN* mRNA has been associated with failures in neuronal excitability (Cochet-Bissuel et al., 2014). We also observed substantial increases in the expression of extracellular matrix (EM) modulators such as *MMP13*, *EFEMP1* and *FMOD* (Jan et al., 2016; Li et al., 2022; Livingstone et al., 2020) during the early trans-differentiation process. While the peripheral secretion of growth factors and cytokines is likely advantageous for the therapeutic potential of MSCs (Han et al., 2022; Liang et al., 2021) the paracrine action of proteins including the EM modulators (Hu et al., 2012; Inoue et al., 2010; Sengupta et al., 2022) still raises concerns about their tumorigenic potential.

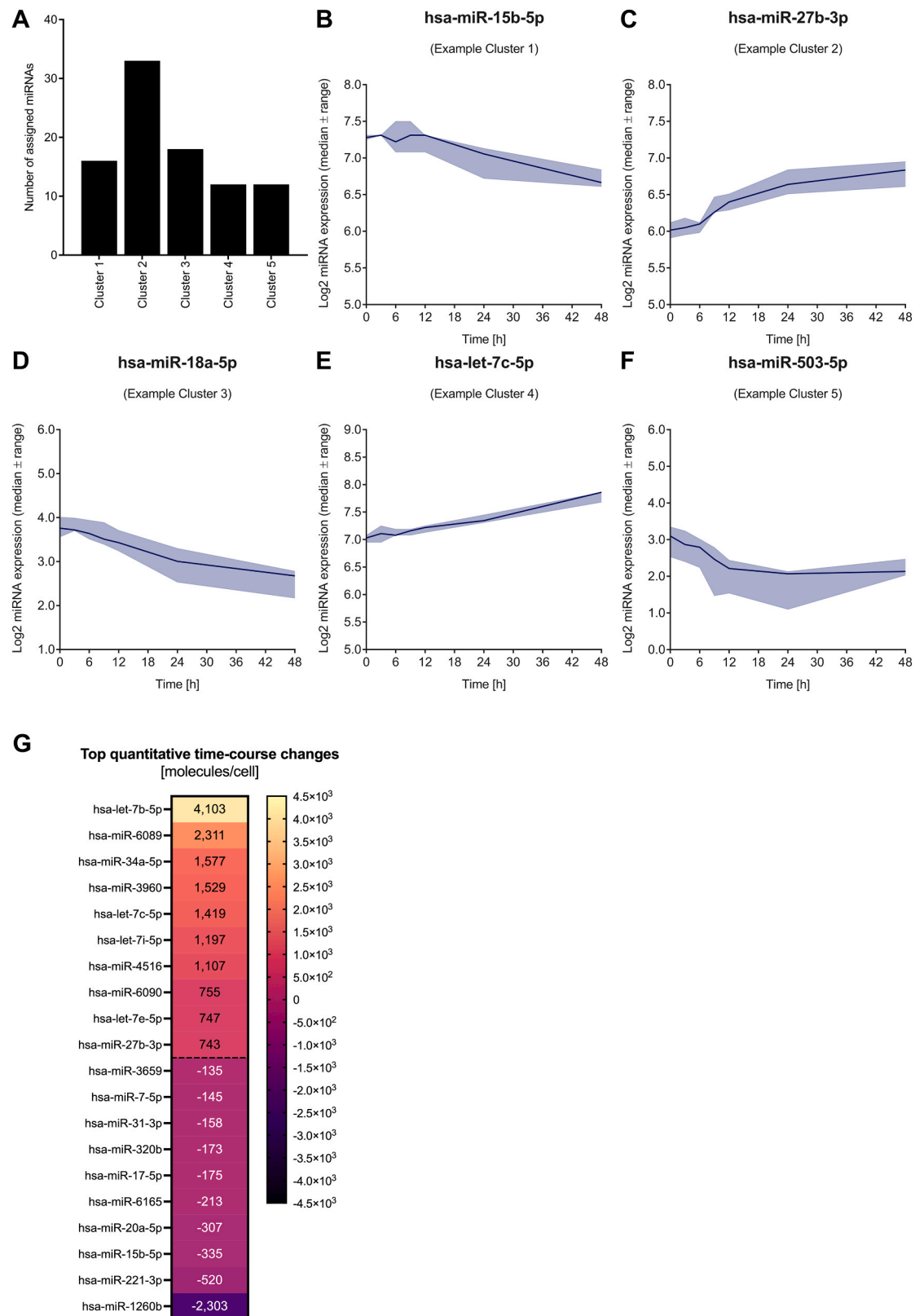


**Fig. 7.** Representation of prominently altered microRNAs by five clusters of time-course expression trajectories and quantitative overview on the highest miRNA expression changes. A: For 91 prominently altered microRNAs (miRNAs, miRs) the different shapes of time-course expression trajectories were represented by five distinct clusters. An overview on the number of miRNAs that have been assigned to each of the clusters is depicted. B-F: Representative expression trajectories are exemplarily illustrated by miR-15b-5p (B), miR-27b-3p (C), miR-18a-5p (D), let-7c-5p (E) and miR-503-5p (F), respectively. Log<sub>2</sub> expression data are shown as median results (line) with total ranges (filled areas) of the four replicated time-course experiments. G: As the result of quantitative evaluation, molecular changes are depicted for the most altered miRNAs. Maximum time-course changes are represented for the top 10 decreasing and increasing miRNAs, respectively. Separation between these groups is indicated by the black dashed horizontal line.

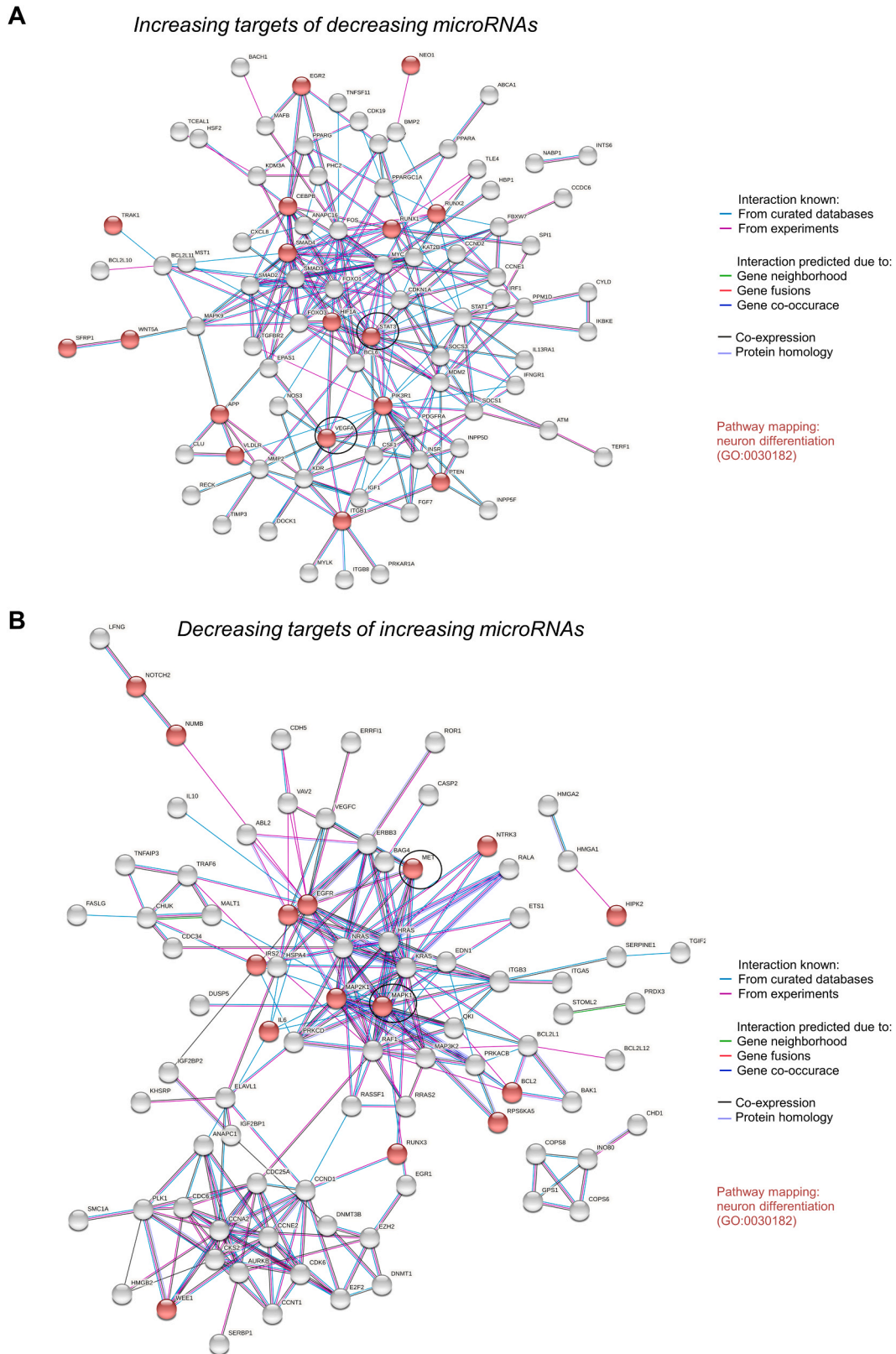


**Fig. 8.** Networks of miRNA-target interactions. Validated miRNA-target interactions were matched with time-resolved RNA expression data. Including the 91 prominently altered miRNAs, inverse directions of time-course expression patterns were assumed for their targeted transcripts. The represented networks, showing functional interactions between the resulting targets, were generated and exported from the STRING database. Networks are represented for the increasing targets of decreasing miRNAs (A) and the decreasing targets of increasing miRNAs (B), respectively. Targets that showed a connection to the GO term "neuron differentiation" are highlighted in red and exemplary targets at central nodes of the networks are identified by black circles.

In the CNS, neural stem cells (NSCs) originating from the embryonic ectoderm, give rise to both neurons and glia cells (Kennea and Mehmet, 2002; Tang et al., 2017). Similarly, MSCs have been described to possess the capability to trans-differentiate into these cell types (Urrutia et al., 2019). As for the expression dynamics of neural and glial signatures, we found ambiguous characteristics of neurons, astrocytes and oligodendrocytes upon the *in vitro* neurogenic trans-differentiation process. These different characteristics may be explained by a mixed cell population comprising neurons and glial cells. A similar scenario has previously been reported for umbilical cord derived MSCs (UC-MSCs). After stimulation of the UC-MSCs with neuronal conditioned medium for up to 12 days, expression of some glial proteins was observed in a portion of the trans-differentiated cells (Fu et al., 2004). Remarkably, our protein staining analyses revealed heterogeneity in the distribution of certain protein markers among the cells, indicating distinct cellular variability (Freeman et al., 2015). Future projects could benefit from more detailed insights into the composition of trans-differentiated cell populations, potentially using single-cell transcriptome or flow cytometric analyses.

It is also conceivable that the ambiguous marker characteristics reflect an uncompleted cell type differentiation. Various transcripts that are associated with the maintenance of stemness showed decreasing expression levels during the time-course, including genes such as *BIRC5* (Gil-Kulik et al., 2019), *HMMR* (Tilghman et al., 2014) and *MYB* (Malaterre et al., 2008). On the other hand, somatic stemness markers such as *KLF4* or *MYC* (Qin et al., 2011; Zaytseva et al., 2020; Zhao et al., 2017) exhibited an unexpected expression increase. Reduced expression of further stemness markers, as for example *NEK2*, has previously been linked to inefficient neural differentiation and the persistence of pluripotency (Spice et al., 2022). In addition, we were able to detect NSC specific genes throughout the trans-differentiation process, for example nestin that was detectable even up to 7 days, as validated by protein staining analyses. Overall, our findings and other reports on a later lineage conversion of terminally differentiated MSCs (Song and Tuan, 2004) imply the maintenance of a residual stem cell capacity. This should be acknowledged when assessing the utility of MSC-derived neurons for the transplantation into critical tissues like the CNS. Future studies should focus on a comprehensive assessment of persistent stem cell characteristics in the resulting neuron-like cells. Further transcriptomic analysis will be necessary during first hours after transplantation to decipher the directions of those cells in an *in vivo* environment. Potential strategies to mitigate tumorigenicity and stemness persistence will depend on results of transcriptomic analysis of cells isolated from *in vivo* experiments.

In summary, our time-resolved RNA profiling provides a comprehensive view on the transcriptomic landscape during the early MSC trans-differentiation process and highlights functional links to the acquisition of neuronal features. The assessment of experimentally validated target interactions together with the time-resolved RNA expression data indicate an essential role of microRNA mediated post-transcriptional regulations in the early MSC trans-differentiation. The combination of MSC identity markers shows that RNA signatures contribute to distinguish between the native MSC cell state and an emerging neurogenic trans-differentiation. Our data further indicate potential safety risks of MSC-derived neurons by showing an expression of common tumorigenic factors and the maintenance of stem cell characteristics.

#### Ethics approval and informed consent

Not applicable.

#### Author contributions

C.D., E.M. and U.F. designed the study; K.T., C.D. and U.F. performed the experiments; A.E., C.D., K.T., M.H., A.K. and U.F. analyzed and visualized the data; C.D., E.M., A.E., A.K., and U.F. wrote the

manuscript; all authors edited and approved the final manuscript.

#### Funding

This research was supported by the Hans-und-Ruth-Giessen-Stiftung (2021) and the Hedwig-Stalter-Stiftung (2022) to Diener C.

#### CRediT authorship contribution statement

**Eckart Meese:** Writing – original draft, Conceptualization. **Ulrike Fischer:** Writing – original draft, Formal analysis, Data curation, Conceptualization. **Andreas Keller:** Writing – review & editing, Formal analysis. **Caroline Diener:** Writing – original draft, Formal analysis, Data curation, Conceptualization. **Konstantin Thüre:** Formal analysis, Data curation. **Annika Engel:** Writing – original draft, Formal analysis. **Martin Hart:** Formal analysis.

#### Declaration of Generative AI and AI-assisted technologies in the writing process

The authors disclose that they did not use AI and AI-assisted technologies in the writing process.

#### Declaration of Competing Interest

The authors declare that they have no known competing financial interests or personal relationships that could have appeared to influence the work reported in this paper.

#### Appendix A. Supporting information

Supplementary data associated with this article can be found in the online version at [doi:10.1016/j.ejcb.2024.151458](https://doi.org/10.1016/j.ejcb.2024.151458).

#### References

- Alles, J., Fehlmann, T., Fischer, U., Backes, C., Galata, V., Minet, M., Hart, M., Abu-Halima, M., Grasser, F.A., Lenhof, H.P., Keller, A., Meese, E., 2019. An estimate of the total number of true human miRNAs. *Nucleic Acids Res* 47, 3353–3364. <https://doi.org/10.1093/nar/gkz097>.
- Alsubait, A., Aldossary, W., Rashid, M., Algamdi, A., Alrfaei, B.M., 2020. CYP1B1 gene: Implications in glaucoma and cancer. *J. Cancer* 11, 4652–4661. <https://doi.org/10.7150/jca.42669>.
- Aranha, M.M., Santos, D.M., Sola, S., Steer, C.J., Rodrigues, C.M., 2011. miR-34a regulates mouse neural stem cell differentiation. *PLoS One* 6, e21396. <https://doi.org/10.1371/journal.pone.0021396>.
- Augustyniak, J., Lenart, J., Zychowicz, M., Stepien, P.P., Buzanska, L., 2017. Mitochondrial biogenesis and neural differentiation of human iPSC is modulated by idebenone in a developmental stage-dependent manner. *Biogerontology* 18, 665–677. <https://doi.org/10.1007/s10522-017-9718-4>.
- Bar-Joseph, Z., Gitter, A., Simon, I., 2012. Studying and modelling dynamic biological processes using time-series gene expression data. *Nat. Rev. Genet* 13, 552–564. <https://doi.org/10.1038/nrg3244>.
- Bartoszewski, R., Sikorski, A.F., 2018. Editorial focus: entering into the non-coding RNA era. *Cell Mol. Biol. Lett.* 23, 45. <https://doi.org/10.1186/s11658-018-0111-3>.
- Bergsland, M., Werme, M., Malewicz, M., Perlmann, T., Muhr, J., 2006. The establishment of neuronal properties is controlled by Sox4 and Sox11. *Genes Dev.* 20, 3475–3486. <https://doi.org/10.1101/gad.403406>.
- Boone, D.K., Weisz, H.A., Bi, M., Falduto, M.T., Torres, K.E.O., Willey, H.E., Volsko, C.M., Kumar, A.M., Micci, M.A., Dewitt, D.S., Prough, D.S., Hellmich, H.L., 2017. Evidence linking microRNA suppression of essential prosurvival genes with hippocampal cell death after traumatic brain injury. *Sci. Rep.* 7, 6645. <https://doi.org/10.1038/s41598-017-06341-6>.
- Cai, N., Kurachi, M., Shibasaki, K., Okano-Uchida, T., Ishizaki, Y., 2012. CD44-positive cells are candidates for astrocyte precursor cells in developing mouse cerebellum. *Cerebellum* 11, 181–193. <https://doi.org/10.1007/s12311-011-0294-x>.
- Chapouton, P., Skupien, P., Hesel, B., Coolen, M., Moore, J.C., Madelaine, R., Kremmer, E., Faus-Kessler, T., Blader, P., Lawson, N.D., Bally-Cuif, L., 2010. Notch activity levels control the balance between quiescence and recruitment of adult neural stem cells. *J. Neurosci.* 30, 7961–7974. <https://doi.org/10.1523/JNEUROSCI.6170-09.2010>.
- Choudhary, P., Gupta, A., Singh, S., 2021. Therapeutic advancement in neuronal transdifferentiation of mesenchymal stromal cells for neurological disorders. *J. Mol. Neurosci.* 71, 889–901. <https://doi.org/10.1007/s12031-020-01714-5>.

- Cline, H., 2005. Synaptogenesis: a balancing act between excitation and inhibition. *Curr. Biol.* 15, R203–R205. <https://doi.org/10.1016/j.cub.2005.03.010>.
- Coccini, T., Schicchi, A., Locatelli, C.A., Caloni, F., Negri, S., Grignani, E., De Simone, U., 2023. Methylglyoxal-induced neurotoxic effects in primary neuronal-like cells transdifferentiated from human mesenchymal stem cells: Impact of low concentrations. *J. Appl. Toxicol.* 43, 1819–1839. <https://doi.org/10.1002/jat.4515>.
- Cochet-Bissuel, M., Lory, P., Monteil, A., 2014. The sodium leak channel, NALCN, in health and disease. *Front Cell Neurosci.* 8, 132. <https://doi.org/10.3389/fncel.2014.00132>.
- Cortes-Medina, L.V., Pasantos-Morales, H., Aguilera-Castrejon, A., Picones, A., Lara-Figueroa, C.O., Luis, E., Montesinos, J.J., Cortes-Morales, V.A., De la Rosa Ruiz, M.P., Hernandez-Estevez, E., Bonifaz, L.C., Alvarez-Perez, M.A., Ramos-Mandujano, G., 2019. Neuronal transdifferentiation potential of human mesenchymal stem cells from neonatal and adult sources by a small molecule cocktail. *Stem Cells Int* 2019, 7627148. <https://doi.org/10.1155/2019/7627148>.
- Coulthard, L.G., Hawksworth, O.A., Li, R., Balachandran, A., Lee, J.D., Sepehrband, F., Kurniawan, N., Jeanes, A., Simmons, D.G., Wolvetang, E., Woodruff, T.M., 2017. Complement C5aR1 signaling promotes polarization and proliferation of embryonic neural progenitor cells through PKCzeta. *J. Neurosci.* 37, 5395–5407. <https://doi.org/10.1523/JNEUROSCI.0525-17.2017>.
- Cunniff, C., Bassetti, J.A., Ellis, N.A., 2017. Bloom's syndrome: clinical spectrum, molecular pathogenesis, and cancer predisposition. *Mol. Syndr.* 8, 4–23. <https://doi.org/10.1159/000452082>.
- Diener, C., Hart, M., Kehl, T., Rheinheimer, S., Ludwig, N., Krammes, L., Pawusch, S., Lenhof, K., Tänzler, T., Schub, D., Sester, M., Walch-Rückheim, B., Keller, A., Lenhof, H.P., Meese, E., 2020. Quantitative and time-resolved miRNA pattern of early human T cell activation. *Nucleic Acids Res* 48, 10164–10183. <https://doi.org/10.1093/nar/gkaa788>.
- Diener, C., Hart, M., Kehl, T., Becker-Dorison, A., Tänzler, T., Schub, D., Krammes, L., Sester, M., Keller, A., Unger, M., Walch-Rückheim, B., Lenhof, H.P., Meese, E., 2023a. Time-resolved RNA signatures of CD4+ T cells in Parkinson's disease. *Cell Death Discov.* 9, 18. <https://doi.org/10.1038/s41420-023-01333-0>.
- Diener, C., Keller, A., Meese, E., 2022. Emerging concepts of miRNA therapeutics: from cells to clinic. *Trends Genet* 38, 613–626. <https://doi.org/10.1016/j.tig.2022.02.006>.
- Diener, C., Keller, A., Meese, E., 2023b. The miRNA-target interactions: An underestimated intricacy. *Nucleic Acids Res.* <https://doi.org/10.1093/nar/gkad1142>.
- Diener, C., Keller, A., Meese, E., 2024. The miRNA-target interactions: an underestimated intricacy. *Nucleic Acids Res* 52, 1544–1557. <https://doi.org/10.1093/nar/gkad1142>.
- Dominici, M., Le Blanc, K., Mueller, I., Slaper-Cortenbach, I., Marini, F., Krause, D., Deans, R., Keating, A., Prockop, D., Horwitz, E., 2006. Minimal criteria for defining multipotent mesenchymal stromal cells. The International Society for Cellular Therapy position statement. *Cytotherapy* 8, 315–317. <https://doi.org/10.1080/14653240600855905>.
- Elias, G.M., Elias, L.A., Apostolides, P.F., Kriegstein, A.R., Nicoll, R.A., 2008. Differential trafficking of AMPA and NMDA receptors by SAP102 and PSD-95 underlies synapse development. *Proc. Natl. Acad. Sci. USA* 105, 20953–20958. <https://doi.org/10.1073/pnas.0811025106>.
- Fan, X., Fu, Y., Zhou, X., Sun, L., Yang, M., Wang, M., Chen, R., Wu, Q., Yong, J., Dong, J., Wen, L., Qiao, J., Wang, X., Tang, F., 2020. Single-cell transcriptome analysis reveals cell lineage specification in temporal-spatial patterns in human cortical development. *Sci. Adv.* 6, eaaz2978. <https://doi.org/10.1126/sciadv.aaz2978>.
- Farioli-Vecchioli, S., Tirone, F., 2015. Control of the cell cycle in adult neurogenesis and its relation with physical exercise. *Brain Plast.* 1, 41–54. <https://doi.org/10.3233/BPL-150013>.
- Fawal, M.A., Davy, A., 2018. Impact of metabolic pathways and epigenetics on neural stem cells. *Epigenet Insights* 11, 2516865718820946. <https://doi.org/10.1177/2516865718820946>.
- Feier, A.M., Portan, D., Manu, D.R., Kostopoulos, V., Kotrotsos, A., Strnad, G., Dobreaun, M., Salcudean, A., Bataga, T., 2022. Primary MSCs for personalized medicine: ethical challenges, isolation and biocompatibility evaluation of 3D electrospun and printed scaffolds. *Biomedicines* 10. <https://doi.org/10.3390/biomedicines10071563>.
- Filiano, A.J., Xu, Y., Tustison, N.J., Marsh, R.L., Baker, W., Smirnov, I., Overall, C.C., Gadani, S.P., Turner, S.D., Weng, Z., Peerzade, S.N., Chen, H., Lee, K.S., Scott, M.M., Beenhakker, M.P., Litvak, V., Kipnis, J., 2016. Unexpected role of interferon-gamma in regulating neuronal connectivity and social behaviour. *Nature* 535, 425–429. <https://doi.org/10.1038/nature18626>.
- Freeman, B.T., Jung, J.P., Ogle, B.M., 2015. Single-cell RNA-seq of bone marrow-derived mesenchymal stem cells reveals unique profiles of lineage priming. *PLoS One* 10, e0136199. <https://doi.org/10.1371/journal.pone.0136199>.
- Fu, Y.S., Shih, Y.T., Cheng, Y.C., Min, M.Y., 2004. Transformation of human umbilical mesenchymal cells into neurons in vitro. *J. Biomed. Sci.* 11, 652–660. <https://doi.org/10.1007/BF02256131>.
- Fuchs, H., Theuser, M., Wruck, W., Adjaye, J., 2014. miR-27 negatively regulates pluripotency-associated genes in human embryonal carcinoma cells. *PLoS One* 9, e111637. <https://doi.org/10.1371/journal.pone.0111637>.
- Funa, K., Sasahara, M., 2014. The roles of PDGF in development and during neurogenesis in the normal and diseased nervous system. *J. Neuroimmune Pharm.* 9, 168–181. <https://doi.org/10.1007/s11481-013-9479-z>.
- Furutachi, S., Matsumoto, A., Nakayama, K.I., Gotoh, Y., 2013. p57 controls adult neural stem cell quiescence and modulates the pace of lifelong neurogenesis. *EMBO J.* 32, 970–981. <https://doi.org/10.1038/emboj.2013.50>.
- Fusco, C.M., Desch, K., Dorbaum, A.R., Wang, M., Staab, A., Chan, I.C.W., Vail, E., Villier, V., Langer, J.D., Schuman, E.M., 2021. Neuronal ribosomes exhibit dynamic and context-dependent exchange of ribosomal proteins. *Nat. Commun.* 12, 6127. <https://doi.org/10.1038/s41467-021-26365-x>.
- Gan, K., Dong, G.H., Wang, N., Zhu, J.F., 2020. miR-221-3p and miR-222-3p downregulation promoted osteogenic differentiation of bone marrow mesenchyme stem cells through IGF-1/ERK pathway under high glucose condition. *Diabetes Res Clin. Pr.* 167, 108121. <https://doi.org/10.1016/j.diabres.2020.108121>.
- Gebert, L.F.R., MacRae, I.J., 2019. Regulation of microRNA function in animals. *Nat. Rev. Mol. Cell Biol.* 20, 21–37. <https://doi.org/10.1038/s41580-018-0045-7>.
- Gil-Kulik, P., Krzyzanowski, A., Dudzinska, E., Karwat, J., Chomik, P., Swistowska, M., Kondracka, A., Kwasniewska, A., Cioch, M., Joczuk, M., Nogalski, A., Kocki, J., 2019. Potential involvement of BIRC5 in maintaining pluripotency and cell differentiation of human stem cells. *Oxid. Med Cell Longev.* 2019, 8727925. <https://doi.org/10.1155/2019/8727925>.
- Gomez de San Jose, N., Massa, F., Halbgebauer, S., Oeckl, P., Steinacker, P., Otto, M., 2022. Neuronal pentraxins as biomarkers of synaptic activity: from physiological functions to pathological changes in neurodegeneration. *J. Neural Transm. (Vienna)* 129, 207–230. <https://doi.org/10.1007/s00702-021-02411-2>.
- Gorjala, P., Cairncross, J.G., Gary, R.K., 2016. p53-dependent up-regulation of CDKN1A and down-regulation of CCNE2 in response to beryllium. *Cell Prolif.* 49, 698–709. <https://doi.org/10.1111/cpr.12291>.
- Greene, L.A., Tischler, A.S., 1976. Establishment of a noradrenergic clonal line of rat adrenal pheochromocytoma cells which respond to nerve growth factor. *Proc. Natl. Acad. Sci. USA* 73, 2424–2428. <https://doi.org/10.1073/pnas.73.7.2424>.
- Guo, H., Ingolia, N.T., Weissman, J.S., Bartel, D.P., 2010. Mammalian microRNAs predominantly act to decrease target mRNA levels. *Nature* 466, 835–840. <https://doi.org/10.1038/nature09267>.
- Hamada, N., Fujita, Y., Kojima, T., Kitamoto, A., Akao, Y., Nozawa, Y., Ito, M., 2012. MicroRNA expression profiling of NGF-treated PC12 cells revealed a critical role for miR-221 in neuronal differentiation. *Neurochem Int* 60, 743–750. <https://doi.org/10.1016/j.neuint.2012.03.010>.
- Hamby, M.E., Coskun, V., Sun, Y.E., 2008. Transcriptional regulation of neuronal differentiation: the epigenetic layer of complexity. *Biochim Biophys. Acta* 1779, 432–437. <https://doi.org/10.1016/j.bbaggm.2008.07.006>.
- Han, Y., Yang, J., Fang, J., Zhou, Y., Candi, E., Wang, J., Hua, D., Shao, C., Shi, Y., 2022. The secretion profile of mesenchymal stem cells and potential applications in treating human diseases. *Signal Transduct. Target Ther.* 7, 92. <https://doi.org/10.1038/s41392-022-00932-0>.
- Hardwick, L.J., Ali, F.R., Azzarelli, R., Philpott, A., 2015. Cell cycle regulation of proliferation versus differentiation in the central nervous system. *Cell Tissue Res* 359, 187–200. <https://doi.org/10.1007/s00441-014-1895-8>.
- Harris, D.T., 2014. Stem cell banking for regenerative and personalized medicine. *Biomedicines* 2, 50–79. <https://doi.org/10.3390/biomedicines2010050>.
- Harris, M.A., Clark, J., Ireland, A., Lomax, J., Ashburner, M., Foulger, R., Eilbeck, K., Lewis, S., Marshall, B., Mungall, C., Richter, J., Rubin, G.M., Blake, J.A., Bult, C., Dolan, M., Drabkin, H., Eppig, J.T., Hill, D.P., Ni, L., Ringwald, M., Balakrishnan, R., Cherry, J.M., Christie, K.R., Costanzo, M.C., Dwight, S.S., Engel, S., Fisk, D.G., Hirschman, J.E., Hong, E.L., Hong, R.S., Suthuraman, A., Theesfeld, C.L., Botstein, D., Dolinski, K., Feierbach, B., Berardini, T., Mundodi, S., Rhee, S.Y., Apweiler, R., Barrell, D., Camon, E., Dimmer, E., Lee, V., Chisholm, R., Gaudet, P., Kibbe, W., Kishore, R., Schwarz, E.M., Sternberg, P., Gwinn, M., Hannick, L., Wortman, J., Berriman, M., Wood, V., de la Cruz, N., Tonellato, P., Jaiswal, P., Seigfried, T., White, R., Gene Ontology, C., 2004. The Gene Ontology (GO) database and informatics resource. *Nucleic Acids Res* 32, D258–D261. <https://doi.org/10.1093/nar/gkh036>.
- He, Y., Cai, Y., Pai, P.M., Ren, X., Xia, Z., 2021. The causes and consequences of miR-503 dysregulation and its impact on cardiovascular disease and cancer. *Front Pharm.* 12, 629611. <https://doi.org/10.3389/fphar.2021.629611>.
- He, Z., Hu, X., Liu, W., Dorrance, A., Garzon, R., Houghton, P.J., Shen, C., 2017. P53 suppresses ribonucleotide reductase via inhibiting mTORC1. *Oncotarget* 8, 41422–41431. <https://doi.org/10.18632/oncotarget.17440>.
- Hermann, A., Gastl, R., Liebau, S., Popa, M.O., Fiedler, J., Boehm, B.O., Maisel, M., Lerche, H., Schwarz, J., Brenner, R., Storch, A., 2004. Efficient generation of neural stem cell-like cells from adult human bone marrow stromal cells. *J. Cell Sci.* 117, 4411–4422. <https://doi.org/10.1242/jcs.01307>.
- Hernandez, R., Jimenez-Luna, C., Perales-Adan, J., Perazzoli, G., Melguizo, C., Prados, J., 2020. Differentiation of human mesenchymal stem cells towards neuronal lineage: clinical trials in nervous system disorders. *Biomol. Ther.* 28, 34–44. <https://doi.org/10.4062/biomolther.2019.065>.
- Hmadcha, A., Martin-Montalvo, A., Gauthier, B.R., Soria, B., Capilla-Gonzalez, V., 2020. Therapeutic potential of mesenchymal stem cells for cancer therapy. *Front Bioeng. Biotechnol.* 8, 43. <https://doi.org/10.3389/fbioe.2020.00043>.
- Hoang, D.M., Pham, P.T., Bach, T.Q., Ngo, A.T.L., Nguyen, Q.T., Phan, T.T.K., Nguyen, G.H., Le, P.T.T., Hoang, V.T., Forsyth, N.R., Heke, M., Nguyen, L.T., 2022. Stem cell-based therapy for human diseases. *Signal Transduct. Target Ther.* 7, 272. <https://doi.org/10.1038/s41392-022-01134-4>.
- Hong, Y.R., Lee, H., Park, M.H., Lee, J.K., Lee, J.Y., Suh, H.D., Jeong, M.S., Bae, J.S., Jin, H.K., 2015. CCL2 induces neural stem cell proliferation and neuronal differentiation in Niemann-Pick type C mice. *J. Vet. Med Sci.* 77, 693–699. <https://doi.org/10.1292/jvms.14-0352>.
- Hu, B., Nandhu, M.S., Sim, H., Agudelo-Garcia, P.A., Saldívar, J.C., Dolan, C.E., Mora, M.E., Nuovo, G.J., Cole, S.E., Viapiano, M.S., 2012. Fibulin-3 promotes glioma growth and resistance through a novel paracrine regulation of Notch signaling. *Cancer Res* 72, 3873–3885. <https://doi.org/10.1158/0008-5472.CAN-12-1060>.

- Huang, W., Bhaduri, A., Velmeshev, D., Wang, S., Wang, L., Rottkamp, C.A., Alvarez-Buylla, A., Rowitch, D.H., Kriegstein, A.R., 2020. Origins and proliferative states of human oligodendrocyte precursor cells. *e511 Cell* 182, 594–608. <https://doi.org/10.1016/j.cell.2020.06.027>.
- Huang, F., Chen, L., Guo, W., Huang, T., Cai, Y.D., 2022. Identification of human cell cycle phase markers based on single-cell RNA-Seq data by using machine learning methods. *Biomed. Res Int* 2022, 2516653. <https://doi.org/10.1155/2022/2516653>.
- Inoue, A., Takahashi, H., Harada, H., Kohno, S., Ohue, S., Kobayashi, K., Yano, H., Tanaka, J., Ohnishi, T., 2010. Cancer stem-like cells of glioblastoma characteristically express MMP-13 and display highly invasive activity. *Int. J. Oncol.* 37, 1121–1131. <https://doi.org/10.3892/ijo.00000764>.
- Jan, A.T., Lee, E.J., Choi, L., 2016. Fibromodulin: a regulatory molecule maintaining cellular architecture for normal cellular function. *Int. J. Biochem. Cell Biol.* 80, 66–70. <https://doi.org/10.1016/j.biocel.2016.09.023>.
- Jandial, R., Singec, L., Ames, C.P., Snyder, E.Y., 2008. Genetic modification of neural stem cells. *Mol. Ther.* 16, 450–457. <https://doi.org/10.1038/sj.mt.6300402>.
- Jiao, Y., Palmgren, B., Novozhilova, E., Englund Johansson, U., Spieles-Engemann, A.L., Kale, A., Stupp, S.I., Olivius, P., 2014. BDNF increases survival and neuronal differentiation of human neural precursor cells cotransplanted with a nanofiber gel to the auditory nerve in a rat model of neuronal damage. *Biomed. Res Int* 2014, 356415. <https://doi.org/10.1155/2014/356415>.
- Kennea, N.L., Mehmet, H., 2002. Neural stem cells. *J. Pathol.* 197, 536–550. <https://doi.org/10.1002/path.1189>.
- Kern, F., Aparicio-Puerta, E., Li, Y., Fehlmann, T., Kehl, T., Wagner, V., Ray, K., Ludwig, N., Lenhof, H.P., Meese, E., Keller, A., 2021a. miRTargetLink 2.0-interactive miRNA target gene and target pathway network. *Nucleic Acids Res* 49, W409–W416. <https://doi.org/10.1093/nar/gkab297>.
- Kern, F., Krammes, L., Danz, K., Diener, C., Kehl, T., Kuchler, O., Fehlmann, T., Kahraman, M., Rheinheimer, S., Aparicio-Puerta, E., Wagner, S., Ludwig, N., Backes, C., Lenhof, H.P., von Briesen, H., Hart, M., Keller, A., Meese, E., 2021b. Validation of human microRNA target pathways enables evaluation of target prediction tools. *Nucleic Acids Res* 49, 127–144. <https://doi.org/10.1093/nar/gkaa1161>.
- Khan, A.A., Huat, T.J., Al Mutery, A., El-Serafi, A.T., Kacem, H.H., Abdallah, S.H., Reza, M.F., Abdullah, J.M., Jaafar, H., 2020. Significant transcriptomic changes are associated with differentiation of bone marrow-derived mesenchymal stem cells into neural progenitor-like cells in the presence of bFGF and EGF. *Cell Biosci.* 10, 126. <https://doi.org/10.1186/s13578-020-00487-z>.
- Kopen, G.C., Prockop, D.J., Phinney, D.G., 1999. Marrow stromal cells migrate throughout forebrain and cerebellum, and they differentiate into astrocytes after injection into neonatal mouse brains. *Proc. Natl. Acad. Sci. USA* 96, 10711–10716. <https://doi.org/10.1073/pnas.96.19.10711>.
- Krueger, D.D., Tuffy, L.P., Papadopoulos, T., Brose, N., 2012. The role of neurexins and neuroligins in the formation, maturation, and function of vertebrate synapses. *Curr. Opin. Neurobiol.* 22, 412–422. <https://doi.org/10.1016/j.comb.2012.02.012>.
- Kwon, S.E., Chapman, E.R., 2011. Synaptophysin regulates the kinetics of synaptic vesicle endocytosis in central neurons. *Neuron* 70, 847–854. <https://doi.org/10.1016/j.neuron.2011.04.001>.
- Lee, D.Y., Lee, S.E., Kwon, D.H., Nithiyandam, S., Lee, M.H., Hwang, J.S., Basith, S., Ahn, J.H., Shin, T.H., Lee, G., 2021. Strategies to improve the quality and freshness of human bone marrow-derived mesenchymal stem cells for neurological diseases. *Stem Cells Int* 2021, 8444599. <https://doi.org/10.1155/2021/8444599>.
- Li, P., Li, H.X., Jiang, H.Y., Zhu, L., Wu, H.Y., Li, J.T., Lai, J.H., 2017. Expression of NG2 and platelet-derived growth factor receptor alpha in the developing neonatal rat brain. *Neural Regen. Res* 12, 1843–1852. <https://doi.org/10.4103/1673-5374.219045>.
- Li, S., Pritchard, D.M., Yu, L.G., 2022. Regulation and function of matrix metalloproteinase-13 in cancer progression and metastasis. *Cancers* 14. <https://doi.org/10.3390/cancers14133263>.
- Liang, W., Chen, X., Zhang, S., Fang, J., Chen, M., Xu, Y., Chen, X., 2021. Mesenchymal stem cells as a double-edged sword in tumor growth: focusing on MSC-derived cytokines. *Cell Mol. Biol. Lett.* 26, 3. <https://doi.org/10.1186/s11658-020-00246-5>.
- Liu, Q., Cheng, G., Wang, Z., Zhan, S., Xiong, B., Zhao, X., 2015. Bone marrow-derived mesenchymal stem cells differentiate into nerve-like cells in vitro after transfection with brain-derived neurotrophic factor gene. *Vitr. Cell Dev. Biol. Anim.* 51, 319–327. <https://doi.org/10.1007/s11626-015-9875-1>.
- Liu, Y., Jiang, X., Zhang, X., Chen, R., Sun, T., Fok, K.L., Dong, J., Tsang, L.L., Yi, S., Ruan, Y., Guo, J., Yu, M.K., Tian, Y., Chung, Y.W., Yang, M., Xu, W., Chung, C.M., Li, T., Chan, H.C., 2011. Dedifferentiation-reprogrammed mesenchymal stem cells with improved therapeutic potential. *Stem Cells* 29, 2077–2089. <https://doi.org/10.1002/stem.764>.
- Livingstone, I., Uversky, V.N., Furniss, D., Wiberg, A., 2020. The pathophysiological significance of fibulin-3. *Biomolecules* 10. <https://doi.org/10.3390/biom10091294>.
- Lukomska, B., Stanaszek, L., Zuba-Surma, E., Legosz, P., Sarzynska, S., Drela, K., 2019. Challenges and controversies in human mesenchymal stem cell therapy. *Stem Cells Int* 2019, 9628536. <https://doi.org/10.1155/2019/9628536>.
- Malaterre, J., Mantamadiotis, T., Dworkin, S., Lightowler, S., Yang, Q., Ransome, M.I., Turnley, A.M., Nichols, N.R., Emambokos, N.R., Frampton, J., Ramsay, R.G., 2008. c-Myb is required for neural progenitor cell proliferation and maintenance of the neural stem cell niche in adult brain. *Stem Cells* 26, 173–181. <https://doi.org/10.1634/stemcells.2007-0293>.
- Mao, S., Li, H., Sun, Q., Zen, K., Zhang, C.Y., Li, L., 2014. miR-17 regulates the proliferation and differentiation of the neural precursor cells during mouse corticogenesis. *FEBS J.* 281, 1144–1158. <https://doi.org/10.1111/febs.12680>.
- McKenzie, A.T., Wang, M., Hauberg, M.E., Fullard, J.F., Kozlenkov, A., Keenan, A., Hurd, Y.L., Dracheva, S., Casaccia, P., Roussos, P., Zhang, B., 2018. Brain cell type specific gene expression and co-expression network architectures. *Sci. Rep.* 8, 8868. <https://doi.org/10.1038/s41598-018-27293-5>.
- McKinnon, P.J., 2013. Maintaining genome stability in the nervous system. *Nat. Neurosci.* 16, 1523–1529. <https://doi.org/10.1038/nm.3537>.
- Mertsch, S., Schurgers, L.J., Weber, K., Paulus, W., Senner, V., 2009. Matrix gla protein (MGP): an overexpressed and migration-promoting mesenchymal component in glioblastoma. *BMC Cancer* 9, 302. <https://doi.org/10.1186/1471-2407-9-302>.
- Miao, Z., Sun, H., Xue, Y., 2017. Isolation and characterization of human chorionic membranes mesenchymal stem cells and their neural differentiation. *Tissue Eng. Regen. Med* 14, 143–151. <https://doi.org/10.1007/s13770-017-0025-6>.
- Migliorini, E., Ban, J., Greci, G., Andolfi, L., Pozzato, A., Tormen, M., Torre, V., Lazzarino, M., 2013. Nanomechanics controls neuronal precursors adhesion and differentiation. *Biotechnol. Bioeng.* 110, 2301–2310. <https://doi.org/10.1002/bit.24880>.
- Minguell, J.J., Fierro, F.A., Epanan, M.J., Elices, A.A., Sierralta, W.D., 2005. Nonstimulated human uncommitted mesenchymal stem cells express cell markers of mesenchymal and neural lineages. *Stem Cells Dev.* 14, 408–414. <https://doi.org/10.1089/scd.2005.14.408>.
- Monaco, E., Bionaz, M., Rodriguez-Zas, S., Hurley, W.L., Wheeler, M.B., 2012. Transcriptomics comparison between porcine adipose and bone marrow mesenchymal stem cells during in vitro osteogenic and adipogenic differentiation. *PLoS One* 7, e32481. <https://doi.org/10.1371/journal.pone.0032481>.
- Monte, M., Benetti, R., Buscemi, G., Sandy, P., Del Sal, G., Schneider, C., 2003. The cell cycle-regulated protein human GTSE-1 controls DNA damage-induced apoptosis by affecting p53 function. *J. Biol. Chem.* 278, 30356–30364. <https://doi.org/10.1074/jbc.M302902200>.
- Morimoto, K., Nakajima, K., 2019. Role of the Immune System in the Development of the Central Nervous System. *Front. Neurosci.* 13, 916. <https://doi.org/10.3389/fnins.2019.00916>.
- Musial-Wysocka, A., Kot, M., Majka, M., 2019. The pros and cons of mesenchymal stem cell-based therapies. *Cell Transpl.* 28, 801–812. <https://doi.org/10.1177/0963689719837897>.
- Nango, H., Kosuge, Y., Yoshimura, N., Miyagishi, H., Kanazawa, T., Hashizaki, K., Suzuki, T., Ishige, K., 2020. The molecular mechanisms underlying prostaglandin d (2)-induced neurogenesis in motor neuron-like NSC-34 cells. *Cells* 9. <https://doi.org/10.3390/cells9040934>.
- Oguma, Y., Kuroda, Y., Wakao, S., Kushida, Y., Dezawa, M., 2022. Single-cell RNA sequencing reveals different signatures of mesenchymal stromal cell pluripotent-like and multipotent populations. *iScience* 25, 105395. <https://doi.org/10.1016/j.isci.2022.105395>.
- Oikari, L.E., Okolicsanyi, R.K., Griffiths, L.R., Haupt, L.M., 2016a. Data defining markers of human neural stem cell lineage potential. *Data Brief* 7, 206–215. <https://doi.org/10.1016/j.dib.2016.02.030>.
- Oikari, L.E., Okolicsanyi, R.K., Qin, A., Yu, C., Griffiths, L.R., Haupt, L.M., 2016b. Cell surface heparan sulfate proteoglycans as novel markers of human neural stem cell fate determination. *Stem Cell Res* 16, 92–104. <https://doi.org/10.1016/j.scr.2015.12.011>.
- Pelkey, K.A., Barksdale, E., Craig, M.T., Yuan, X., Sukumaran, M., Vargish, G.A., Mitchell, R.M., Wyeth, M.S., Petralia, R.S., Chittajallu, R., Karlsson, R.M., Cameron, H.A., Murata, Y., Colonnese, M.T., Worley, P.F., McBain, C.J., 2015. Pentraxins coordinate excitatory synapse maturation and circuit integration of parvalbumin interneurons. *Neuron* 85, 1257–1272. <https://doi.org/10.1016/j.neuron.2015.02.020>.
- Pittenger, M.F., Discher, D.E., Peault, B.M., Phinney, D.G., Hare, J.M., Caplan, A.L., 2019. Mesenchymal stem cell perspective: cell biology to clinical progress. *NPJ Regen. Med* 4, 22. <https://doi.org/10.1038/s41536-019-0083-6>.
- Poon, V.Y., Gu, M., Ji, F., VanDongen, A.M., Fivaz, M., 2016. miR-27b shapes the presynaptic transcriptome and influences neurotransmission by silencing the polycomb group protein Bmi1. *BMC Genom.* 17, 777. <https://doi.org/10.1186/s12864-016-3139-7>.
- Qin, S., Liu, M., Niu, W., Zhang, C.L., 2011. Dysregulation of Kruppel-like factor 4 during brain development leads to hydrocephalus in mice. *Proc. Natl. Acad. Sci. USA* 108, 21117–21121. <https://doi.org/10.1073/pnas.1112351109>.
- Quinn, L.M., Herr, A., McGarry, T.J., Richardson, H., 2001. The Drosophila Geminin homolog: roles for Geminin in limiting DNA replication, in anaphase and in neurogenesis. *Genes Dev.* 15, 2741–2754. <https://doi.org/10.1101/gad.916201>.
- Rahbaran, M., Zekiy, A.O., Bahramali, M., Jahangir, M., Mardasi, M., Sakhaei, D., Thangavelu, L., Shomali, N., Zamani, M., Mohammadi, A., Rahnama, N., 2022. Therapeutic utility of mesenchymal stromal cell (MSC)-based approaches in chronic neurodegeneration: a glimpse into underlying mechanisms, current status, and prospects. *Cell Mol. Biol. Lett.* 27, 56. <https://doi.org/10.1186/s11658-022-00359-z>.
- Ramos, J., Fu, D., 2019. The emerging impact of tRNA modifications in the brain and nervous system. *Biochim. Biophys. Acta Gene Regul. Mech.* 1862, 412–428. <https://doi.org/10.1016/j.bbagr.2018.11.007>.
- Roharf, F., Mason, E.A., Matigian, N., Mosbergen, R., Korn, O., Chen, T., Butcher, S., Patel, J., Atkinson, K., Khosrotehrani, K., Fisk, N.M., Le Cao, K.A., Wells, C.A., 2016. A molecular classification of human mesenchymal stromal cells. *PeerJ* 4, e1845. <https://doi.org/10.7717/peerj.1845>.
- Rohban, R., Pieber, T.R., 2017. Mesenchymal stem and progenitor cells in regeneration: tissue specificity and regenerative potential. *Stem Cells Int* 2017, 5173732. <https://doi.org/10.1155/2017/5173732>.
- Roush, S., Slack, F.J., 2008. The let-7 family of microRNAs. *Trends Cell Biol.* 18, 505–516. <https://doi.org/10.1016/j.tcb.2008.07.007>.
- Ruijtenberg, S., van den Heuvel, S., 2016. Coordinating cell proliferation and differentiation: antagonism between cell cycle regulators and cell type-specific gene

- expression. *Cell Cycle* 15, 196–212. <https://doi.org/10.1080/15384101.2015.1120925>.
- Sakry, D., Yigit, H., Dimou, L., Trotter, J., 2015. Oligodendrocyte precursor cells synthesize neuromodulatory factors. *PLoS One* 10, e0127222. <https://doi.org/10.1371/journal.pone.0127222>.
- Schmitz, U., Lai, X., Winter, F., Wolkenhauer, O., Vera, J., Gupta, S.K., 2014. Cooperative gene regulation by microRNA pairs and their identification using a computational workflow. *Nucleic Acids Res* 42, 7539–7552. <https://doi.org/10.1093/nar/gku465>.
- Scolz, M., Widlund, P.O., Piazza, S., Bublik, D.R., Reber, S., Peche, L.Y., Ciani, Y., Hubner, N., Isokane, M., Monte, M., Ellenberg, J., Hyman, A.A., Schneider, C., Bird, A.W., 2012. GTSE1 is a microtubule plus-end tracking protein that regulates EB1-dependent cell migration. *PLoS One* 7, e51259. <https://doi.org/10.1371/journal.pone.0051259>.
- Selbach, M., Schwanhauser, B., Thierfelder, N., Fang, Z., Khanin, R., Rajewsky, N., 2008. Widespread changes in protein synthesis induced by microRNAs. *Nature* 455, 58–63. <https://doi.org/10.1038/nature07228>.
- Semprich, C.I., Davidson, L., Amorim Torres, A., Patel, H., Briscoe, J., Metzis, V., Storey, K.G., 2022. ERK1/2 signalling dynamics promote neural differentiation by regulating chromatin accessibility and the polycomb repressive complex. *PLoS Biol.* 20, e3000221. <https://doi.org/10.1371/journal.pbio.3000221>.
- Sengupta, S., Mondal, M., Prasavi, K.R., Mukherjee, A., Magod, P., Urbach, S., Friedmann-Morvinski, D., Marin, P., Somasundaram, K., 2022. Differentiated glioma cell-derived fibromodulin activates integrin-dependent Notch signaling in endothelial cells to promote tumor angiogenesis and growth. *Elife* 11. <https://doi.org/10.7554/eLife.78972>.
- Shaltouki, A., Peng, J., Liu, Q., Rao, M.S., Zeng, X., 2013. Efficient generation of astrocytes from human pluripotent stem cells in defined conditions. *Stem Cells* 31, 941–952. <https://doi.org/10.1002/stem.1334>.
- Shefchek, K.A., Harris, N.L., Gargano, M., Matentzoglou, N., Unni, D., Brush, M., Keith, D., Conlin, T., Vasilevsky, N., Zhang, X.A., Balhoff, J.P., Babb, L., Bello, S.M., Blau, H., Bradford, Y., Carbon, S., Carmody, L., Chan, L.E., Cipriani, V., Cuzick, A., Della Rocca, M., Dunn, N., Essaid, S., Fey, P., Grove, C., Gouridine, J.P., Hamosh, A., Harris, M., Helbig, I., Hoatlin, M., Joachimiak, M., Jupp, S., Lett, K.B., Lewis, S.E., McNamara, C., Pendlington, Z.M., Pilgrim, C., Putman, T., Ravanmehr, V., Reese, J., Riggs, E., Robb, S., Roncaglia, P., Seager, J., Segerdell, E., Similuk, M., Storm, A.L., Thaxon, C., Thessen, A., Jacobsen, J.O.B., McMurry, J.A., Groza, T., Kohler, S., Smedley, D., Robinson, P.N., Mungali, C.J., Haendel, M.A., Munoz-Torres, M.C., Osumi-Sutherland, D., 2020. The Monarch Initiative in 2019: an integrative data and analytic platform connecting phenotypes to genotypes across species. *Nucleic Acids Res* 48, D704–D715. <https://doi.org/10.1093/nar/gkz997>.
- Shi, Z., Geng, Y., Liu, J., Zhang, H., Zhou, L., Lin, Q., Yu, J., Zhang, K., Liu, J., Gao, X., Zhang, C., Yao, Y., Zhang, C., Sun, Y.E., 2018. Single-cell transcriptomics reveals gene signatures and alterations associated with aging in distinct neural stem/progenitor cell subpopulations. *Protein Cell* 9, 351–364. <https://doi.org/10.1007/s13238-017-0450-2>.
- Snyder, M., Huang, X.Y., Zhang, J.J., 2011. Stat3 is essential for neuronal differentiation through direct transcriptional regulation of the Sox6 gene. *FEBS Lett.* 585, 148–152. <https://doi.org/10.1016/j.febslet.2010.11.030>.
- Song, L., Tuan, R.S., 2004. Transdifferentiation potential of human mesenchymal stem cells derived from bone marrow. *FASEB J.* 18, 980–982. <https://doi.org/10.1096/fj.03-1100fj>.
- Spice, D.M., Cooper, T.T., Lajoie, G.A., Kelly, G.M., 2022. Never in Mitosis Kinase 2 regulation of metabolism is required for neural differentiation. *Cell Signal* 100, 110484. <https://doi.org/10.1016/j.celsig.2022.110484>.
- Spurgat, M.S., Tang, S.J., 2022. Single-Cell RNA-sequencing: astrocyte and microglial heterogeneity in health and disease. *Cells* 11. <https://doi.org/10.3390/cells11132021>.
- Sun, Y.M., Cooper, M., Finch, S., Lin, H.H., Chen, Z.F., Williams, B.P., Buckley, N.J., 2008. Rest-mediated regulation of extracellular matrix is crucial for neural development. *PLoS One* 3, e3656. <https://doi.org/10.1371/journal.pone.0003656>.
- Szklarczyk, D., Gable, A.L., Nastou, K.C., Lyon, D., Kirsch, R., Pyysalo, S., Doncheva, N. T., Legeay, M., Fang, T., Bork, P., Jensen, L.J., von Mering, C., 2021. The STRING database in 2021: customizable protein-protein networks, and functional characterization of user-uploaded gene/measurement sets. *Nucleic Acids Res* 49, D605–D612. <https://doi.org/10.1093/nar/gkaa1074>.
- Tang, S., Xie, Z., Wang, P., Li, J., Wang, S., Liu, W., Li, M., Wu, X., Su, H., Cen, S., Ye, G., Zheng, G., Wu, Y., Shen, H., 2019. LncRNA-OG promotes the osteogenic differentiation of bone marrow-derived mesenchymal stem cells under the regulation of hnRNPK. *Stem Cells* 37, 270–283. <https://doi.org/10.1002/stem.2937>.
- Tang, Y., Yu, P., Cheng, L., 2017. Current progress in the derivation and therapeutic application of neural stem cells. *Cell Death Dis.* 8, e3108. <https://doi.org/10.1038/cddis.2017.504>.
- Thanaskody, K., Jusop, A.S., Tye, G.J., Wan Kamarul Zaman, W.S., Dass, S.A., Nordin, F., 2022. MSCs vs. iPSCs: Potential in therapeutic applications. *Front Cell Dev. Biol.* 10, 1005926. <https://doi.org/10.3389/fcell.2022.1005926>.
- Theis, V., Theiss, C., 2018. VEGF - a stimulus for neuronal development and regeneration in the CNS and PNS. *Curr. Protein Pept. Sci.* 19, 589–597. <https://doi.org/10.2174/1389203719666180104113937>.
- Thomas, A., Gasque, P., Vaudry, D., Gonzalez, B., Fontaine, M., 2000. Expression of a complete and functional complement system by human neuronal cells in vitro. *Int Immunol.* 12, 1015–1023. <https://doi.org/10.1093/intimm/12.7.1015>.
- Tilghman, J., Wu, H., Sang, Y., Shi, X., Guerrero-Cazares, H., Quinones-Hinojosa, A., Eberhart, C.G., Latterra, J., Ying, M., 2014. HMMR maintains the stemness and tumorigenicity of glioblastoma stem-like cells. *Cancer Res* 74, 3168–3179. <https://doi.org/10.1158/0008-5472.CAN-13-2103>.
- Tondreau, T., Lagneau, L., Dejeneffe, M., Massy, M., Mortier, C., Delforge, A., Bron, D., 2004. Bone marrow-derived mesenchymal stem cells already express specific neural proteins before any differentiation. *Differentiation* 72, 319–326. <https://doi.org/10.1111/j.1432-0436.2004.07207003.x>.
- Urrutia, D.N., Caviedes, P., Mardones, R., Minguell, J.J., Vega-Letter, A.M., Jofre, C.M., 2019. Comparative study of the neural differentiation capacity of mesenchymal stromal cells from different tissue sources: an approach for their use in neural regeneration therapies. *PLoS One* 14, e0213032. <https://doi.org/10.1371/journal.pone.0213032>.
- Varoqueaux, F., Aramuni, G., Rawson, R.L., Mohrmann, R., Missler, M., Gottmann, K., Zhang, W., Sudhof, T.C., Brose, N., 2006. Neuroligins determine synapse maturation and function. *Neuron* 51, 741–754. <https://doi.org/10.1016/j.neuron.2006.09.003>.
- Vasanthan, J., Gurusamy, N., Rajasingh, S., Sigamani, V., Kirankumar, S., Thomas, E.L., Rajasingh, J., 2020. Role of Human Mesenchymal Stem Cells in Regenerative Therapy. *Cells* 10. <https://doi.org/10.3390/cells10010054>.
- Volarevic, V., Markovic, B.S., Gazdic, M., Volarevic, A., Jovicic, N., Arsenijevic, N., Armstrong, L., Djonov, V., Lako, M., Stojkovic, M., 2018. Ethical and safety issues of stem cell-based therapy. *Int J. Med Sci.* 15, 36–45. <https://doi.org/10.7150/ijms.21666>.
- Wada, T., Haigh, J.J., Ema, M., Hitoshi, S., Chaddah, R., Rossant, J., Nagy, A., van der Kooy, D., 2006. Vascular endothelial growth factor directly inhibits primitive neural stem cell survival but promotes definitive neural stem cell survival. *J. Neurosci.* 26, 6803–6812. <https://doi.org/10.1523/JNEUROSCI.0526-06.2006>.
- Walsh, P., Truong, V., Hill, C., Stoflet, N.D., Baden, J., Low, W.C., Keirstead, S.A., Dutton, J.R., Parr, A.M., 2017. Defined culture conditions accelerate small-molecule-assisted neural induction for the production of neural progenitors from human-induced pluripotent stem cells. *Cell Transpl.* 26, 1890–1902. <https://doi.org/10.1177/0963689717737074>.
- Wang, Z., Chai, C., Wang, R., Feng, Y., Huang, L., Zhang, Y., Xiao, X., Yang, S., Zhang, Y., Zhang, X., 2021. Single-cell transcriptome atlas of human mesenchymal stem cells exploring cellular heterogeneity. *Clin. Transl. Med* 11, e650. <https://doi.org/10.1002/ctm2.650>.
- van Wietmarschen, N., Merzouk, S., Halsema, N., Spierings, D.C.J., Guryev, V., Lansdorp, P.M., 2018. BLM helicase suppresses recombination at G-quadruplex motifs in transcribed genes. *Nat. Commun.* 9, 271. <https://doi.org/10.1038/s41467-017-02760-1>.
- Xia, X., Wang, Y., Zheng, J.C., 2022. The microRNA-17 ~ 92 family as a key regulator of neurogenesis and potential regenerative therapeutics of neurological disorders. *Stem Cell Rev. Rep.* 18, 401–411. <https://doi.org/10.1007/s12015-020-10050-5>.
- Xiong, Y., Zhang, Y., Xiong, S., Williams-Villalobo, A.E., 2020. A glance of p53 functions in brain development, neural stem cells, and brain cancer. *Biology* 9. <https://doi.org/10.3390/biology9090285>.
- Yao, S., 2016. MicroRNA biogenesis and their functions in regulating stem cell potency and differentiation. *Biol. Proced. Online* 18, 8. <https://doi.org/10.1186/s12575-016-0037-y>.
- Ylivinkka, I., Sihto, H., Tynneninen, O., Hu, Y., Laakso, A., Kivisaari, R., Laakkonen, P., Keski-Oja, J., Hyytiäinen, M., 2017. Motility of glioblastoma cells is driven by netrin-1 induced gain of stemness. *J. Exp. Clin. Cancer Res* 36, 9. <https://doi.org/10.1186/s13046-016-0482-0>.
- Zaytseva, O., Kim, N.H., Quinn, L.M., 2020. MYC in brain development and cancer. *Int J. Mol. Sci.* 21. <https://doi.org/10.3390/ijms21207742>.
- Zhang, Z., Ma, Z., Zou, W., Guo, H., Liu, M., Ma, Y., Zhang, L., 2019. The appropriate marker for astrocytes: comparing the distribution and expression of three astrocytic markers in different mouse cerebral regions. *Biomed. Res Int* 2019, 9605265. <https://doi.org/10.1155/2019/9605265>.
- Zhao, W., Li, Y., Zhang, X., 2017. Stemness-related markers in cancer. *Cancer Transl. Med* 3, 87–95. <https://doi.org/10.4103/ctm.ctm.69.16>.
- Zhao, C., Sun, G., Li, S., Lang, M.F., Yang, S., Li, W., Shi, Y., 2010. MicroRNA let-7b regulates neural stem cell proliferation and differentiation by targeting nuclear receptor TLX signaling. *Proc. Natl. Acad. Sci. USA* 107, 1876–1881. <https://doi.org/10.1073/pnas.0908750107>.
- Zheng, B., Wang, C., He, L., Xu, X., Qu, J., Hu, J., Zhang, H., 2013. Neural differentiation of mesenchymal stem cells influences chemotactic responses to HGF. *J. Cell Physiol.* 228, 149–162. <https://doi.org/10.1002/jcp.24114>.
- Zheng, K., Wang, C., Yang, J., Huang, H., Zhao, X., Zhang, Z., Qiu, M., 2018. Molecular and genetic evidence for the PDGFRalpha-independent population of oligodendrocyte progenitor cells in the developing mouse brain. *J. Neurosci.* 38, 9505–9513. <https://doi.org/10.1523/JNEUROSCI.1510-18.2018>.
- Zhou, Y., He, C.H., Herzog, E.L., Peng, X., Lee, C.M., Nguyen, T.H., Gulati, M., Gochuico, B.R., Gahl, W.A., Slade, M.L., Lee, C.G., Elias, J.A., 2015. Chitinase 3-like-1 and its receptors in Hermansky-Pudlak syndrome-associated lung disease. *J. Clin. Invest* 125, 3178–3192. <https://doi.org/10.1172/JCI79792>.